Research Square

Preprints are preliminary reports that have not undergone peer review.
They should not be considered conclusive, used to inform clinical practice,
or referenced by the media as validated information.

Beyond the $CaCl_2$ Brine: Transient Microbial Communities at the Edge of Habitability in lifeless Don Juan Pond, McMurdo Dry Valleys, Antarctica

Francesco Smedile

francesco.smedile@cnr.it

National Research Council

Gina La Spada
National Research Council

Violetta La Cono
National Research Council

Laura Marturano
National Research Council

Francesca Crisafi
National Research Council

Maurizio Azzaro
National Research Council

Nunziatina Porcino
National Research Council

Michele Giani
National Institute of Oceanography and Applied Geophysics

Vincenzo Alessandro Laudicella
National Institute of Oceanography and Applied Geophysics

Luisa Pasti
University of Ferrara

Tatiana Chenet
University of Ferrara

Giacomo Traversa
National Research Council

Biagio Di Mauro
National Research Council

Fabiana Canini
Università degli Studi della Tuscia

Laura Zucconi

Università degli Studi della Tuscia

Michail M. Yakimov

National Research Council

Research Article

Keywords: Don Juan Pond, McMurdo Dry ValleysAntarctica, Calcium chloride-saturated Brines, hypersaline ecosystems, microbial mats, metabarcoding, hyperspectral reflectance, ecological networks, habitability, exoplanetary analogues

Posted Date: November 4th, 2026

DOI: https://doi.org/10.21203/rs.3.rs-11292388/v1

License: This work is licensed under a Creative Commons Attribution 4.0 International License.
Read Full License

Additional Declarations: No competing interests reported.

Beyond the $CaCl_2$ Brine: Transient Microbial Communities at the Edge of Habitability in lifeless Don Juan Pond, McMurdo Dry Valleys, Antarctica

Francesco Smedile[(1)*] ; Gina La Spada[(1)], Violetta La Cono[(1)], Laura Marturano[(1)], Francesca Crisafi[(1)], Maurizio Azzaro[(1)], Nunziatina Porcino[(2)], Michele Giani[(3)], Vincenzo Alessandro Laudicella[(3)], Luisa Pasti[(4)],Tatiana Chenet[(4)], Giacomo Traversa[(1)], Biagio Di Mauro[(1)], Fabiana Canini[(5)], Laura Zucconi[(5)], and Michail M. Yakimov[(1)*]

[(1)]Institute of Polar Sciences, ISP – CNR, Messina, Italy

[(2)] Institute for the Study of Nanostructured Materials, ISMN–CNR, Messina, Italy

[(3)]National Institute of Oceanography and Experimental Geophysics -OGS, Trieste, Italy

[(4)] Department of Environmental and Prevention Sciences, University of Ferrara, Ferrara, Italy

[(5)] Department of Ecological and Biological Sciences, University of Tuscia, Viterbo, Italy

*Corresponding authors: Francesco Smedile, Michail M. YakimovCorrespondence:

Francesco Smedile
francesco.smedile@cnr.it
Gina La Spada
gina.laspada@cnr.it
Violetta La Cono
violetta.lacono@cnr.it
Laura Marturano
laura.marturano@isp.cnr.it
Francesca Crisafi
francesca.crisafi@cnr.it
Maurizio Azzaro
maurizio.azzaro@cnr.it
Nunziatina Porcino
nunziatina.porcino@cnr.it
Michele Giani
mgiani@ogs.it
Vincenzo Alessandro Laudicella
vlaudicella@ogs.it.
Luisa Pasti

luisa.pasti@unife.it
Tatiana Chenet
tatiana.chenet@unife.it
Giacomo Traversa
giacomo.traversa@isp.cnr.it
Biagio Di Mauro
biagio.dimauro@cnr.it
Fabiana Canini
canini.fabiana@unitus.it
Laura Zucconi
zucconi@unitus.it
Michail M. Yakimov
mikhail.iakimov@cnr.it

Abstract

Background

Don Juan Pond (DJP), located in the McMurdo Dry Valleys of Antarctica, is one of the most extreme aquatic environments on Earth due to its $CaCl_2$-rich brines, low water activity, exceptional chaotropicity, subzero temperatures, intense solar radiation, and recurrent desiccation. Although the central DJP brine has long been considered largely inhabitable, the surrounding basin seasonally harbors temporary streams, ponds, and sparse microbial mat. Here, we investigated the diversity, ecological organization, and environmental factor chaping the structure of microbial communities inhabiting these peripheral habitats by integrating hydrochemical analyses, in situ reflectance spectroscopy, DNA metabarcoding, and ecological network analysis.

Results

No DNA suitable for PCR amplification was recovered from the central $CaCl_2$ brine. In contrast, peripheral streams and ponds supported diverse prokaryotic, microeukaryotic,

and fungal communities, with the highest alpha diversity consistently observed in the hydrologically heterogeneous S1 stream system. Prokaryotic assemblages were primarily associated with salinity-related variables, including chlorinity and Mg/Ca ratios, whereas eukaryotic and fungal communities were more strongly correlated with hyperspectral indices indicative of photosynthetic biomass. Transient habitats also hosted micro-metazoans, including rotifers, tardigrades, and nematodes, indicating ecological refugia capable of sustaining complex trophic interactions under polyextreme conditions. Hyperspectral indices successfully discriminated active microbial mats from inactive sedimentary crusts and were significantly associated with the distribution of multiple bacterial, fungal, and microeukaryotic taxa. Network analyses revealed highly interconnected multi-domain communities composed of bacteria, fungi, algae, protists, and microbial grazers.

Conclusions

The presence of life in the Don Juan Pond basin appears to be largely restricted to temporary habitats supported by seasonal meltwater inputs rather than the central $CaCl_2$ saturated brine itself, which is anathema to all life forms due to a number of strict physicochemical constraints imposed on life. The contrasting responses of prokaryotic and eukaryotic communities suggest that adaptation and persistence represent distinct ecological strategies in this polyextreme ecosystem. These findings indicate that environmental stability may be as important as salinity/chaotropicity in determining habitability limits and demonstrate the value of integrating molecular and hyperspectral approaches to investigate life in extreme terrestrial and exo-planetary analogous environments.

Keywords

(Three to ten keywords representing the main content of the article)

Don Juan Pond; McMurdo Dry ValleysAntarctica; Calcium chloride-saturated Brines; hypersaline ecosystems; microbial mats; metabarcoding; hyperspectral reflectance; ecological networks; habitability; exoplanetary analogues

1. **Background**

The presence of liquid water is considered one of the fundamental prerequisites for the existence of life as we know it, and therefore remains one of the primary criteria in the search for habitable environments beyond Earth [1,2]. However, habitability also depends on a broader set of physicochemical constraints, including temperature, radiation exposure, water activity, salinity, pH, nutrient availability, and energy sources, all of which influence the ability of organisms to survive, even in a quiescent state, and reproduce [3,4]. Consequently, the mere presence of liquid water in an environment does not necessarily imply the existence of active living forms, even if that environment may contain traces of past life. This concept underpins modern astrobiology, within which the detection of liquid water—whether in the present or the past—remains a key criterion in the search for potentially habitable environments on Mars, Europa, Enceladus, and exoplanets located in habitable zones [5,6].

Several natural environments on Earth illustrate this apparent paradox. Among the most notable examples are the $MgCl_2$-rich athalassohaline Deep Hypersaline Anoxic Basins (DHABs) of the Eastern Mediterranean Sea and Don Juan Pond (DJP) in the McMurdo Dry Valleys of Antarctica, which is filled with a $CaCl_2$-rich brine. Despite their different ionic compositions, both systems are characterized by persistent hypersaline brines of non-marine origin and lie close to the physicochemical limits for life owing to extremely low water activity and intense osmotic and chaotropic stress. Although deep sea, $MgCl_2$-saturated DHABs Discovery, Kryos and Hephaestus are essentially lifeless deserts, their

seawater interfaces host highly specialized microbial communities that have evolved under conditions of stable hypersalinity and chaotropic stress over geological timescales [7–11]. Similarly, the extreme physicochemical conditions of the central $CaCl_2$ brine in DJP are generally considered to completely limit biological activity, and no convincing evidence of active microbial communities has yet been reported from its most concentrated zones [12–14]. Consequently, these systems provide valuable natural laboratories on Planet Earth for investigating the environmental limits of habitability and the ecological mechanisms that enable microbial life to persist under extreme physicochemical constraints.

First described in 1961, Don Juan Pond is a small ice-free hypersaline pond located in the South Fork of Upper Wright Valley, within the McMurdo Dry Valleys of Antarctica [15]. The basin is characterized by $CaCl_2$-rich athalassohaline brines exhibiting exceptionally low water activity and high chaotropicity, together with subzero temperatures, intense solar and ultraviolet radiation, strong katabatic winds, and prolonged periods of desiccation [13,16–18] . The combination of these physicochemical stressors makes DJP one of the most extreme aqueous environments on Earth and one of the closest terrestrial analogues of the cold saline environments inferred to have existed on early Mars [13,19,20] .

The hydrochemistry of DJP has been extensively investigated and indicates that the pond is sustained by $CaCl_2$-rich brines of probable subsurface origin [18,21,22] . Current models suggest that these brines originate from the deliquescence of $CaCl_2$-rich salt deposits, whose highly hygroscopic properties allow the formation and persistence of liquid brines despite the hyperarid conditions of the McMurdo Dry Valleys [13,18]. Surrounding the central brine body, seasonal meltwater coming mainly from adjacent rock glaciers, ephemeral springs and shallow groundwater sporadically forms less saline streams and ponds around the basin [13,21,22] . Although the extreme physicochemical conditions of the central brine are generally considered to severely limit biological activity [12] , microbial mats, algal outcrops and other biological features have been repeatedly observed in the

pond's peripheral aquatic habitats [12,14,23–25]. These observations suggest that seasonal freshwater influxes create temporary ecological refuges capable of supporting microbial communities under conditions significantly less extreme than those prevailing in the central part of the pond, challenging the limits of survival in an otherwise lifeless environment. However, the biodiversity, ecological organization and environmental drivers of these transient communities remain largely unexplored.

Recent advances in DNA metabarcoding have greatly improved our ability to characterize microbial diversity across multiple domains of life, particularly in extreme environments where cultivation-based approaches remain challenging [26,27] . Analyses of prokaryotic (16S rRNA), fungal (ITS2) and microeukaryotic (18S rRNA) markers now provide comprehensive descriptions of microbial community composition and ecological interactions and have been successfully applied to Antarctic terrestrial ecosystems, including the McMurdo Dry Valleys [28–30].Recent studies further indicate that environmental gradients, particularly salinity, may differently shape prokaryotic, fungal and microeukaryotic communities through distinct community assembly mechanisms, suggesting that different microbial groups may exhibit contrasting ecological responses along the same environmental gradients [31].

In parallel, hyperspectral reflectance spectroscopy has emerged as a rapid and non-destructive approach for detecting photosynthetic biomass, pigment composition and biological activity in Antarctic microbial mats. By exploiting subtle variations in reflectance associated with photosynthetic pigments, hyperspectral analyses have successfully characterized biological soil crusts [32] and microbial communities across Antarctic regions [30]. The integration of molecular and hyperspectral approaches therefore offers the opportunity to investigate both microbial diversity and functional indicators of biological activity across extreme environmental gradients.

In this study, we investigated the biodiversity, ecological organization and environmental drivers of microbial communities inhabiting transient aquatic habitats surrounding Don Juan Pond. To address these knowledge gaps, we adopted a polyphasic approach combining hydrochemical characterization, *in situ* hyperspectral reflectance analyses, DNA metabarcoding targeting prokaryotic, fungal and microeukaryotic communities (16S rRNA, ITS2 and 18S rRNA), and ecological network analyses. Specifically, we aimed to (i) characterize the taxonomic diversity associated with microbial mats and adjacent sediments, (ii) identify the environmental and spectral variables shaping community composition, (iii) evaluate the potential of hyperspectral indices as proxies for biological activity, and (iv) assess whether the observed communities reflect long-term adaptation to extreme conditions or persistence within transient ecological refugia. We hypothesized that biologically active communities would be primarily associated with transient meltwater habitats rather than with the central $CaCl_2$ brine of the pond, reflecting the existence of temporary ecological refugia, and that prokaryotic, fungal and microeukaryotic communities would exhibit distinct ecological responses to the strong environmental gradients characterizing the basin.

2. Materials and Methods

2.1 Study area and field campaigns

Field activities were conducted within the Don Juan Pond (DJP) basin, Upper Wright Valley, McMurdo Dry Valleys, Antarctica, during two Italian Antarctic Expeditions (PNRA): the XXXVII Expedition (October-December 2021) and the XXXVIII Expedition (November 2022–January 2023). A total of eight field surveys were performed, four during each expedition.

2.2 Sampling strategy

Sampling was designed to encompass the full hydrological gradient of the DJP basin, including the permanent $CaCl_2$-saturated brine as well as the surrounding transient meltwater habitats. Overall, more than 40 water, sediment and ice samples were collected from both the central pond and peripheral streams, ponds and saline deposits. The geographic coordinates, sampling dates, and basic hydrochemical characteristics of the subset of samples selected for complete chemical and biological characterization are provided in the that undergoes a complete chemical and biological analysis Additional file 1. and Supplementary Figure S1.

The two field campaigns covered different phases of the austral summer. While the first expedition was conducted between late October and early December 2021 (Fig.1), the second extended from late November 2022 to early January 2023 (Fig.2). Most importantly, sampling of the biologically active habitats (S1, S2, S3, P1 and P2) was carried out during late December 2022 and early January 2023, corresponding to a more advanced stage of the austral summer, when meltwater production from the adjacent rock glacier was more extensive and transient streams and ponds reached their maximum development. Water and sediment were collected from at least four locations along each stream, and from at least two locations within each pond. Pond P2 was sampled twice over a 35-day interval to evaluate short-term temporal variability. Because DJP is located within Antarctic Specially Managed Area (ASMA) No. 2 (McMurdo Dry Valleys), a protected region of exceptional scientific value, the number of sampling sites and the volume of collected material were minimized in accordance with the environmental permits governing scientific activities in Antarctica, along with precautionary measures to sample aseptically and to avoid polluting the pond and the surrounding area with external microbes and/or other organic and inorganic residue.

2.3 Sampling sites and habitat characterization

The investigated habitats were distributed across the western sector of the DJP basin and included ephemeral streams, shallow ponds, moist sediments, salt-encrusted surfaces and rock-associated niches. Stream S1 originated directly from meltwater draining the western rock glacier and formed a distributed network of shallow channels that later converged into a single stream approximately 80 m long. This system supported the largest and most continuous microbial mats observed during the study and was sampled at 20 locations along its course (samples S1-1 to S1-20). Streams S2 and S3 originated from localized brine seepages within the floodplain. Stream S2 developed from a thin (<2 cm) green water layer into a shallow channel feeding pond P2 before reaching the central basin. Eight samples were collected along this system (samples S2-1 to S2-8) . Stream S3 formed a short (~3 m), shallow fracture-like channel, where visible biological activity was restricted to a thin green biofilm attached to wet rock surfaces. Six samples were collected from this habitat (samples S3-1 to S3-6). Pond P1 consisted of a small isolated pool (~1 m diameter and a few centimeters deep) formed around a rock and showed no visible hydrological connection with the main pond. This pond has been sampled three times (samples P1-1-to P1-3). Similarly to P1, also three samples were obtained from Pond P2 (samples P2-1 to P2-3) a shallow (<5 cm deep) pond approximately 3–5 m wide that received water from stream S2. DNA was only obtained from the first two samples, P2-1 and P2-2. .Orthomosaic surveys were used to document the spatial distribution of sampling sites and to characterize the geomorphological heterogeneity of the investigated area (Fig. S1 additional file 1).

Sediment samples were collected sterilely by using sterile polypropylene spatulas, recovering, whenever possible, a portion of the overlying water together with the uppermost sediment layer in order to preserve the structure of the surface microbial mats. Samples were transferred into sterile 250- or 500-mL polycarbonate bottles (Corning®, USA), taking care to minimize

disturbance of the sediment–water interface and the microbial mat. Following collection, all samples were kept at approximately 4˚C in the dark during field operations and transport to the research station, and were subsequently stored at − 20°C until laboratory processing.

2.4 Environmental measurements

Field measurements included pH, electrical conductivity and salinity, obtained using a portable multiparameter instrument (XS Tester PC 5 – ECOPACK, XS Instruments, Italy) and a handheld refractometer (MASTER-500, Atago, Japan). However, because a thin freshwater layer frequently overlaid sediments saturated with $CaCl_2$-rich brines (Toner et al., 2017), *in situ* salinity measurements were particularly challenging in these environments. Field measurements often varied depending on sampling depth and whether they were performed in the overlying water layer or close to the sediment–microbial mat interface. Therefore, laboratory-based hydrochemical measurements were used for all subsequent statistical analyses.

To avoid cross-contamination among sampling sites, all sampling tools and probes were thoroughly sterilized with 70 % ethanol (vol/vol) and rinsed repeatedly with ultrapure water before each measurement and sample collection.

2.5 Water chemistry

2.5.1 Anions determination by ion chromatography (IC)

For the determination of chloride and sulfate ions, prior to the analysis, brine samples were filtered with PVDF 0.2 µm syringe filters (Agilent Technologies, Santa Clara, CA, USA) and diluted with MilliQ water 1:10000 for Cl^- and 1:100 for SO_4^{2-}. The samples were analyzed with the Dionex Easion Ion Chromatography system (Thermo Scientific, Waltham, MA, USA) equipped with a Dionex ACRS 500 Supressor (4mm), a Dionex IonPac AG22 (4x50

mm) guard column and a Dionex IonPac AS22 (4x250 mm) analytical column. The mobile phase was a solution of Na_2CO_3 4.8 mM and $NaHCO_3$ 1.0 mM with a flow rate of 1.0 mL/min, and the suppressor regenerant was a solution of sulfuric acid 50 mM. The concentrations of Cl^- and SO_4^{2-} were determined by external calibration using multi-analyte standard solutions. Calibration curves showed excellent linearity ($R^2 > 0.999$) over the concentration range of 0.2–25 mg L^{-1}. The limits of detection (LOD) were 0.02 mg L^{-1} for Cl^- and 0.05 mg L^{-1} for SO_4^{2-}. Quality control included the analysis of procedural blanks and matrix-spiked samples, yielding recoveries between 96 and 99%.

2.5.2 Cations determination by flame atomic absorption spectroscopy (FAAS) and inductively coupled plasma mass spectrometry (ICP-MS)

Major cations (Ca, Mg, Na, and K) were quantified by flame atomic absorption spectroscopy (FAAS) using an AAnalyst 800 spectrometer (PerkinElmer, Waltham, MA, USA) equipped with an air–acetylene flame and element-specific hollow cathode lamps. Measurements were carried out at wavelengths of 422.7 nm (Ca), 285.2 nm (Mg), 589.0 nm (Na), and 766.5 nm (K). Brine samples were diluted with Milli-Q water (1:100–1:10,000), depending on the expected analyte concentration. External calibration was performed using TraceCERT® standards (Sigma-Aldrich, Darmstadt, Germany). Calibration curves were linear ($R^2 > 0.999$) within the concentration ranges of 0.5–5 mg L^{-1} for Ca, 0.05–0.5 mg L^{-1} for Mg, 0.1–1 mg L^{-1} for Na, and 0.2–2 mg L^{-1} for K. Limits of detection ranged from 0.02 to 0.05 mg L^{-1}. Analytical quality was assessed through procedural blanks and matrix-spiked samples, resulting in recoveries between 98 and 101%.

Strontium was determined by ICP-MS following filtration through 0.2 µm PVDF syringe filters and dilution (1:10,000) with Milli-Q water. In contrast, Mn and Fe were determined after an off-line solid-phase extraction (SPE) procedure to remove the saline matrix and preconcentrate the analytes. The SPE protocol was adapted from the on-line method

described by Søndergaard et al. (2015). Before use, Chelex-100 resin (Sigma Aldrich, Darmstadt, Germany) was soaked with 5M HCl overnight, filtered on nylon 0.45 µm membrane filter (Sigma Aldrich, Darmstadt, Germany), washed with 2M HNO_3 and MilliQ water and equilibrated with a solution of ammonium acetate 1M at pH 7. 2. For each sample, 2 mL of 2 M ammonium acetate buffer (pH 7.4) was added to 10 mL of brine to adjust the pH to approximately 6. Subsequently, 1g of Chelex-100 resin was added and the suspension was shaken for 1h by using a multi-functional orbital shaker (PSU-20i, Biosan, Riga, Latvia). The resin was then separated by centrifugation (6000 rpm, 10 min), the supernatant discarded, and the resin washed with 10 mL of Milli-Q water to remove residual matrix ions. Adsorbed trace metals were eluted by adding 5 mL of 5% HNO_3 and shaking for an additional 1 h. The eluate was filtered through 0.2 µm PVDF syringe filters, diluted 1:5 with Milli-Q water, and analyzed by ICP-MS. The resin was then separated by centrifugation (6000 rpm, 10 min), the supernatant discarded, and the resin washed with 10 mL of Milli-Q water to remove residual matrix ions. Adsorbed trace metals were eluted by adding 5 mL of 5% HNO_3 and shaking for an additional 1 h. The eluate was filtered through 0.2 µm PVDF syringe filters, diluted 1:5 with Milli-Q water, and analyzed by ICP-MS. The SPE procedure was also applied to procedural blanks, to account for background contamination, and synthetic brines spiked with 10 µg L^{-1} of the analytes to evaluate their recovery which resulted between 91 and 105%.

An Agilent 8800 Triple Quadrupole ICP-MS (Agilent Technologies, Santa Clara, CA, USA) equipped with a MicroMist glass concentric nebulizer, Peltier cooled double-pass Scott-type spray chamber, and Ni cones was used for the analyses. Germanium (Ge) was added to all calibration standards and samples as an internal standard. Instrument operating conditions were as follows:: 1550 W RF power, 8.0 mm sampling depth, 15 L min^{-1} plasma gas, 1.03 L min^{-1} carrier gas, with the spray chamber temperature set at 2°C, 4.5 mL min^{-1} collision gas (He) flow, the monitored isotopes were ^{55}Mn, ^{56}Fe, ^{72}Ge, ^{88}Sr.

The formation of oxides and doubly charged species was checked during the tuning of the instrument by monitoring the CeO^+/Ce^+ and Ce^{2+}/Ce^+ ratios which were optimized at ≤ 1% values. The linearity was verified ($R^2 > 0.999$) over a range of concentration between 0.1 and 200 µg L^{-1}. The LODs were 0.012 µg L^{-1} for Mn, 0.11 µg L^{-1} for Fe, and 0.0085 µg L^{-1} for Sr. Method accuracy was verified through procedural blanks and matrix-spiked samples, yielding recoveries between 96 and 99%.

2.5.3 Thermodynamic modeling and ternary diagrams construction

The raw values were compiled alongside geographic coordinates, sample collection dates, and relevant literature benchmark values to evaluate hydrochemical characteristics across the sampling sites. Thermodynamic modeling and geochemical calculations were performed using the Geochemistry Workbench (GWB) (2026 release 19) software package https://www.gwb.com/downloads.php. To standardize units and assess chemical equilibria, major ion concentrations were converted to molar and molal units, enabling the determination of chlorinity values and water classification types. GWB was further utilized to construct ternary diagrams illustrating relative major ion abundances.

2.6 Hyperspectral reflectance measurements

During the field campaign conducted in January 2023 in DJP, a set of in situ spectroscopy data were collected in correspondence of the surface sampling in order to characterize the optical properties of the surface. Incoming and reflected radiance were measured using a portable spectrometer (Reflectance box, ROX) operating in the visible and near infrared wavelengths (400-900nm) [33]. The instrument features a full width at half maximum of 1.5 nm and subnanometer (0.68nm) spectral sampling. Spectroscopy data collected at DJP were then converted into reflectance [0-1] by normalizing the reflected radiance with the

incoming radiance. We followed the same measurement protocol described in Traversa et al. (2024) [34].

A set of spectral indices was calculated from each reflectance spectrum, including both previously published indices and new indices developed in this study, to summarize the information contained in the spectral data. Specifically, the B6 index was calculated based on the chlorophyll-a absorption band in the 677–681 nm region and the adjacent red edge region in the 696–700 nm range, while the NDVIp (partially normalized difference vegetation index) index was derived from the red and near-infrared (IR) spectral rangesIn particular, B6 was calculated from the chlorophyll-a absorption feature around 677–681 nm and the adjacent red-edge region at 696–700 nm, whereas (a partial normalized difference vegetation index) NDVIp was derived from the red and near-infrared (NIR) spectral domains. Additional spectral indices (D5, D7, and D8) were calculated from wavelength intervals selected on the basis of pigment absorption features and NIR reflectance characteristics identified in the DJP dataset. Indices labelled as (1) were adopted from Levy et al. (2020) [30], indices labelled as (2) were adapted from Di Mauro et al. (2020) [35], whereas indices labelled as (3) were newly proposed in this study based on the analysis of the reflectance spectra collected from the DJP basin.All calculated indices are provided in Additional file 2.

2.7 DNA extraction

DNA extraction was performed using both commercial kits and a phenol–chloroform-based protocol. For an initially screening, several commercial extraction kits were tested, in a first round of extraction attempt, including the DNeasy PowerSoil Pro Kit (Qiagen, UK), the FastDNA SPIN Kit for Soil (MP Biomedicals, UK), and the Zymo Research Quick-DNA Faecal/Soil Microbe MiniPrep Kit (Cambridge Bioscience, UK), following the manufacturers' instructions. However, no amplifiable DNA was obtained from samples collected during the first expedition using these protocols. Preliminary tests on samples

collected during the second expedition with the same commercial kits yielded only limited amounts of DNA. Consequently, all samples from the second expedition were processed using a modified phenol–chloroform extraction protocol based on Zhou et al. (1996) [36]. Briefly, approximately 5 g of sediment containing the surface microbial mat were cryogenically homogenized with sterile quartz sand under liquid nitrogen using three successive freeze–grinding cycles. Cell lysis was performed in CTAB extraction buffer supplemented with proteinase K and SDS, followed by two sequential extractions with chloroform:isoamyl alcohol (24:1). DNA was precipitated with isopropanol, washed with 70% ethanol, air-dried, and finally resuspended in nuclease-free water. DNA concentration was quantified using a Qubit™ 4 Fluorometer (Thermo Fisher Scientific, Waltham, MA, USA), while DNA integrity was assessed by agarose gel electrophoresis.

To assess potential laboratory contamination, an extraction blank was processed in parallel using all reagents, consumables and extraction steps, but without environmental material. The extraction blank was amplified using the three metabarcoding primer sets (16S rRNA, 18S rRNA and ITS), although amplification product was obtained only for the 16S rRNA marker. Further sequence comparison showed that the majority of Amplicon sequence variants (ASVs) detected in the extraction blank were unique to the control, while the few shared ASVs occurred at negligible relative abundances in the environmental samples. Following a conservative decontamination approach, all ASVs detected in the extraction blank were removed from the 16S and ITS datasets before subsequent analyses.

2.8 PCR amplification and sequencing

For prokaryotic community analysis, the V3-V4 variable regions of SSU rRNA gene (S-D-Bact-0341-b-S-17, 5′-CCTACGGGNGGCWGCAG-3′, and S-D-Bact-0785-a-A-21, 5′-GACTACHVGGGTATCTAATCC-3’), hypervariable region of the 16S rRNA gene was amplified using the universal primer as described by Jan Klindworth et al. (2013) [26]. For eukaryotic community analysis, The V9 hypervariable region of the 18S rRNA gene was amplified using the universal primer pair 1380F (5′-CCCTGCCHTTTGTACACAC-3′) and 1510R (5′-CCTTCYGCAGGTTCACCTAC-3′) as described by Amaral-Zettler et al. (2009) [37]. PCR amplicons were sequenced on the Illumina MiSeq platform by Macrogen Inc. Library preparation and sequencing were carried out following standard Illumina protocols [38].

For fungal library preparation, a fragment of the ITS2 genomic region of around 370-440 bp (including primer sequences) was amplified using the primers ITS3 (5’ GCATCGATGAAGAACGCAGC 3’) and ITS4 (5’ TCCTCCGCTTATTGATATGC 3’) [39]. In the first amplification step, PCRs were carried out in a final volume of 12.5 µL, containing 1.25 µL of template DNA, 0.5 µM of the primers, 6.25 µL of Supreme NZYTaq 2x Green Master Mix (NZYTech), and ultrapure water up to 12.5 µL. The reaction mixture was incubated as follows: an initial denaturation step at 95 ºC for 5 min, followed by 35 cycles of 95 ºC for 30 s, 51 °C for 45 s, 72 ºC for 45 s, and a final extension step at 72 ºC for 7 min. The oligonucleotide indices for multiplexing were attached in a second amplification step with identical conditions but only 5 cycles and 60 ºC as the annealing temperature (Vierna et al., 2017). The obtained libraries were purified using the Mag-Bind RXNPure Plus magnetic beads (Omega Bio-tek). Libraries were pooled in equimolar amounts according to the results of a Qubit dsDNA HS Assay (Thermo Fisher Scientific) quantification, and the obtained pools were sequenced in an Illumina NovaSeq platform (PE250). DNA metabarcoding library preparation and sequencing were carried out by AllGenetics & Biology SL (www.allgenetics.eu).

2.9 Bioinformatic analyses Amplicon Sequence Processing, Taxonomic Assignment and Statistical analyses

Raw paired-end FASTQ files were imported into the RStudio package (version 2026.05.1+225), and analyzed using the DADA2 package v. 1.40.0 [40].

After chimeric sequences were removed, taxonomy was assigned to sequence variants using the naive Bayesian classifier method against the Silva Database v138 (v138; https://www.arb-silva.de/documentation/ release-138.2/, and https://zenodo.org/record/4587955#.YgKJlb_MJH4) for prokaryotic organisms and for Eukaryotic organisms Silva v132 (https://zenodo.org/records/10444891)
For the fungal dataset, raw sequences were quality-filtered, trimmed, denoised, merged, and modelled using QIIME2 and DADA2 [41]. Amplicon sequence variants (ASVs) were clustered into Operational Taxonomic Units (OTUs, 97% identity threshold) using vsearch [42] . Representative OTUs (97%) were taxonomically assigned using the UNITE+INSD 8.2 (https://unite.ut.ee/repository.php) database. Only OTUs identified as fungi with an identity threshold of 70% were retained. Diversity analyses were conducted using the phyloseq v. 1.56.0, [43] and the microbiome v 1.34.0 [44].

Alpha diversity was assessed for each sample using the Shannon, Simpson, and Chao1 indices. Beta diversity was evaluated using weighted and unweighted UniFrac distances, as well as Jaccard and Bray–Curtis dissimilarity metrics. Detailed parameters used for sequence filtering and downstream processing are publicly available in the project repository on GitHub (https://github.com/GilSP/Don-Juan-Pond).
Sequence comparison showed that the majority of ASVs detected in the extraction blank were unique to the control, while the few shared ASVs occurred at negligible relative abundances in the environmental samples. Following a conservative decontamination

approach, all ASVs detected in the extraction blank were removed from the 16S and ITS datasets before subsequent analyses.

2.10 Statistical analyses

To investigate the influence of hydrochemical variables and hyperspectral reflectance indices on microbial community structure, a multi-step analytical approach was adopted. Relationships between overall community composition and environmental or spectral variables were first explored using non-metric multidimensional scaling (nMDS) ordinations based on Bray–Curtis dissimilarity matrices, followed by environmental fitting (envfit) and surface fitting (ordisurf) analyses and ANOSIM test implemented in the R package vegan (v2.7-5).

The microbial taxa contributing most to community dissimilarity were subsequently identified using SIMPER (Similarity Percentage) analysis implemented in PAST (PAleontological STatistics; v3.25). Taxa accounting for the largest proportion of beta-diversity (average contribution >0.5% for prokaryotes and >1% for eukaryotes and fungi) were retained for further analyses.

To identify potential associations between dominant microbial groups and environmental or hyperspectral variables, Mantel tests were performed using the R package microeco (v2.2.0) [45]. This combined approach allowed the identification of both the main environmental drivers shaping overall community structure and the specific environmental and spectral variables associated with the distribution of the most influential microbial taxa.

2.11 Network analysis

To investigate co-occurrence patterns among prokaryotes, microbial eukaryotes, and fungi, a multi-domain co-occurrence network was constructed. Prior to network inference, the 16S, 18S, and ITS datasets were independently normalized using the centered log-

ratio (CLR) transformation implemented in the microbiome package. The co-occurrence network was inferred using NetCoMi v. 1.1.0 [46]. Pearson correlations were calculated among ASVs, and non-significant associations were removed using a t-test approach with adaptive Benjamini–Hochberg correction. Network topology and community structure were analysed using the fast greedy clustering algorithm implemented in the netAnalyze function. Singleton nodes were removed prior to network visualization. The network analysis workflow was adapted from [47] . Custom scripts used for network inference and visualization are available in the project repository on GitHub (https://github.com/GIISP/Don-Juan-Pond). All figures were edited and assembled using Inkscape v1.4.4 (Inkscape Project, 2025).

3. Results

3.1 Environmental variability reveals transient microbial habitats

The two field campaigns documented marked temporal variability in the hydrological conditions of the Don Juan Pond (DJP) basin (Fig. 1). During the first survey (2021-2022), the basin evolved from a partially ice-covered lake in early summer to an extensive evaporitic landscape characterized by widespread salt crusts and progressive contraction of the central $CaCl_2$ brine (Fig. 1a–b). In contrast, the second survey (2022-2023) documented the development of several ephemeral meltwater streams and shallow ponds in the western sector of the basin, associated with increased meltwater input from the adjacent rock glacier (Fig. 2). These contrasting hydrological conditions coincided with noticeable differences in the occurrence of biological activity.

During the first campaign, no macroscopic evidence of microbial colonization was observed despite extensive sampling throughout the basin. Furthermore, the minimal

traces of DNA extracted from water, sediment and ice samples did not not contain suitable amplification templates, neitherprokaryotic nor eukaryotic.



Figure 1: DJP basin in the Upper Wright Valley of the McMurdo Dry Valleys in Antarctica.

(a) View of the DJP basin taken in November 2021, showing a significant reduction in pond size and the appearance of extensive deposits of the mineral antarcticite ($CaCl_2.6H_2O$) on the basin floor. (b) The same area photographed in October 2021 from a similar viewpoint, when the pond was partially covered by ice. (c) Localized ice patches observed in November 2022 in the western sector of the basin, close to the rock glacier. These patches indicate the persistence of frozen freshwater or low-salinity water, likely sourced from the adjacent rock glacier, during the austral summer. (d) In January 2023 salt crusts and evaporitic antarticite deposits were discovered accumulating around rocks of various sizes scattered throughout the basin. This highlights the intense evaporation and salt precipitation processes that characterize the DJP environment.

In contrast, the second campaign revealed conspicuous microbial mats associated with localized meltwater habitats (Fig. 2). Three ephemeral streams (S1, S2 and S3) and two

shallow ponds (P1 and P2) supported prominent green, orange and brown microbial mats and were selected for subsequent hydrochemical, hyperspectral and molecular analyses.

Orthomosaic reconstruction highlighted pronounced fine-scale heterogeneity in water availability and substrate characteristics across the western sector of the basin, resulting in a mosaic of temporary aquatic habitats including meltwater tributaries, shallow ponds, wet sediments and salt-encrusted surfaces (Fig. 2). Among the investigated habitats, stream S1 supported the largest and most spatially widespread microbial mats, whereas biological growth in S3 was restricted to a thin biofilm associated with moist rock surfaces. Stream S2 and its associated pond P2 represented an intermediate habitat, while the apparently isolated pond P1 supported localized microbial community.

Macroscopic microbial mats were observed exclusively within streams S1–S3 and ponds P1–P2. However, DNA recovery from stream S3 was insufficient to generate amplicon libraries using any of the primer sets employed; consequently, this site was excluded from all subsequent analyses.

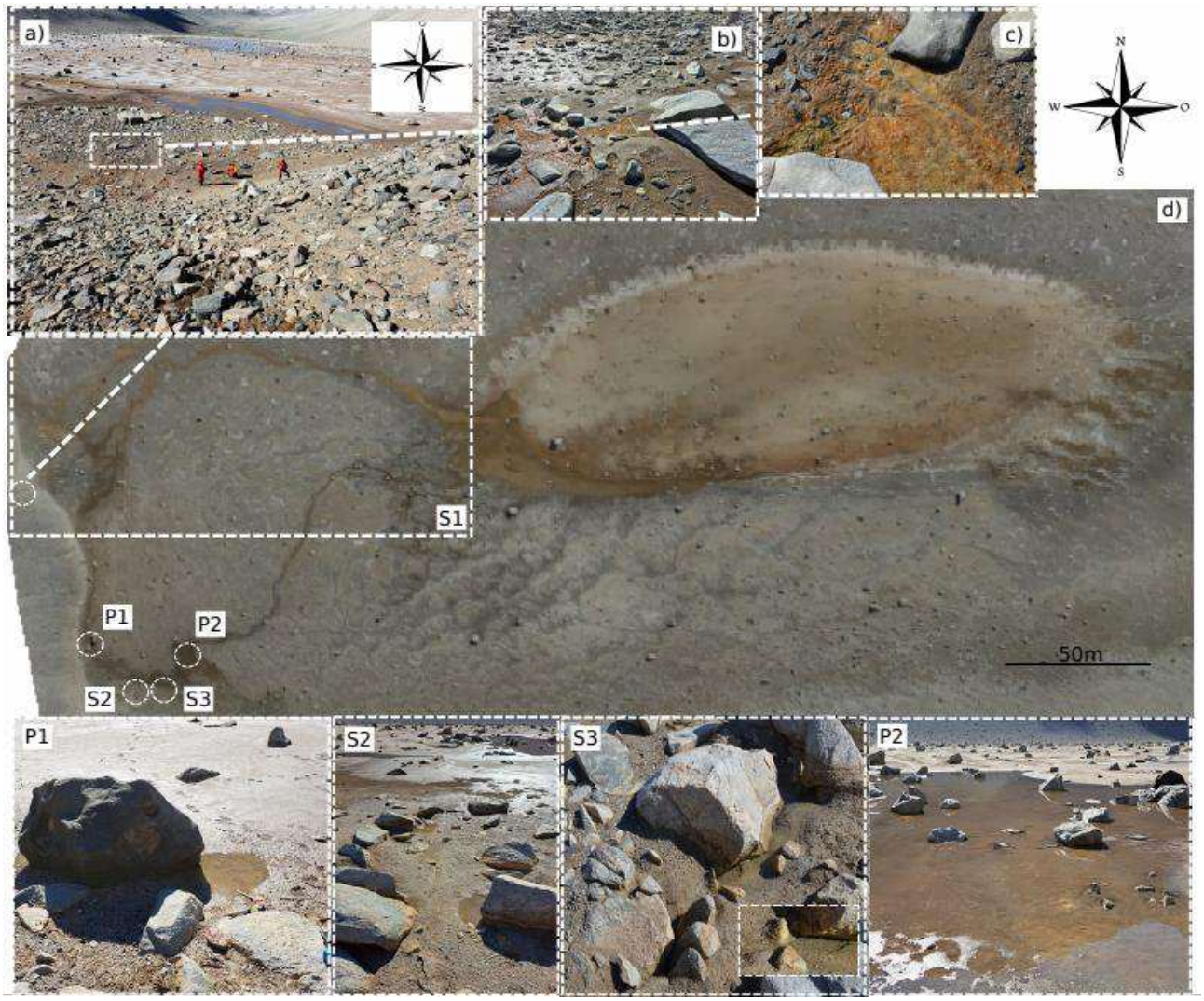


Figure 2. Overview of the DJP basin and sampling sites.

(a) General view of the western sector of the basin showing the location of the studied microbial mat habitats. (b) Close-up of view of the study area characterized by shallow brine channels and wet sediments. (c) Orange-brown microbial mats associated with localized water inflow paths and salt-enriched sediments. (d) Orthomosaic image of the study area showing the distribution of the main sampling sites (P1, P2, S1, S2 and S3). Representative photographs of each sampling site are shown below, highlighting the spatial heterogeneity of substrates, moisture conditions and microbial mat development across the basin, whereas the a), b) and c) are all close up views of the site S1.

Overall, biologically active microbial communities were consistently confined to transient meltwater habitats surrounding the $CaCl_2$ central brine of the pond, whereas neither

macroscopic observations nor molecular analyses revealed any evidence of biological activity in the permanent central brine during all our field expeditions.

3.2 Hydrochemical gradients across transient meltwater habitats

Hydrochemical analyses revealed a pronounced geochemical gradient between the permanent $CaCl_2$-rich brine of Don Juan Pond and the transient meltwater habitats colonized by microbial mats (Fig. 3a,b; Table S1). Although the hydrochemistry of the central basin exhibited moderate temporal variability between the two field campaigns (table S1), its ionic composition remained remarkably stable, with Ca^{2+} and Cl^- consistently representing the dominant cation and anion, respectively. Across all central brine samples, major ions followed the order $Ca^{2+} > Na^+ > Mg^{2+} > K^+$ and $Cl^- > SO_4^{2-}$, in agreement with previous investigations of the DJP basin [18,48,49].

The highest ionic concentrations were measured in the central pond during the 2022 -2023 survey, where Ca^{2+} reached 4.49 mol kg^{-1}, while lower concentrations were recorded in the peripheral sectors of the basin, including the sampling site (Hyppo) located in the southern part of the main basin, sampled during the 2021-2022 campaign (0.56 and 1.78 mol kg^{-1} for Ca^{2+} and Cl^-, respectively). Overall, the chemical composition of the central basin fell within the range previously reported for DJP, despite the substantial temporal variability associated with seasonal changes in hydrological conditions (Additional file 1 and 2 table S1).

In contrast, all habitats supporting visible microbial mats exhibited substantially lower ionic concentrations than the permanent central brine. Ternary diagrams clearly separated the hydrochemical composition of the biologically active streams and ponds (S1, S2, P1 and P2) from that of the central basin (Fig. 3a, b). These peripheral habitats remained dominated by Ca^{2+} and Cl^- but occupied a markedly less concentrated geochemical domain. Average Ca^{2+} concentrations ranged from 0.072 mol kg^{-1} in pond P1 to 0.411 mol

kg⁻¹ in pond P2, whereas average Cl^- concentrations ranged from 0.158 mol kg⁻¹ in P1 to 2.109 mol kg⁻¹ in stream S1.

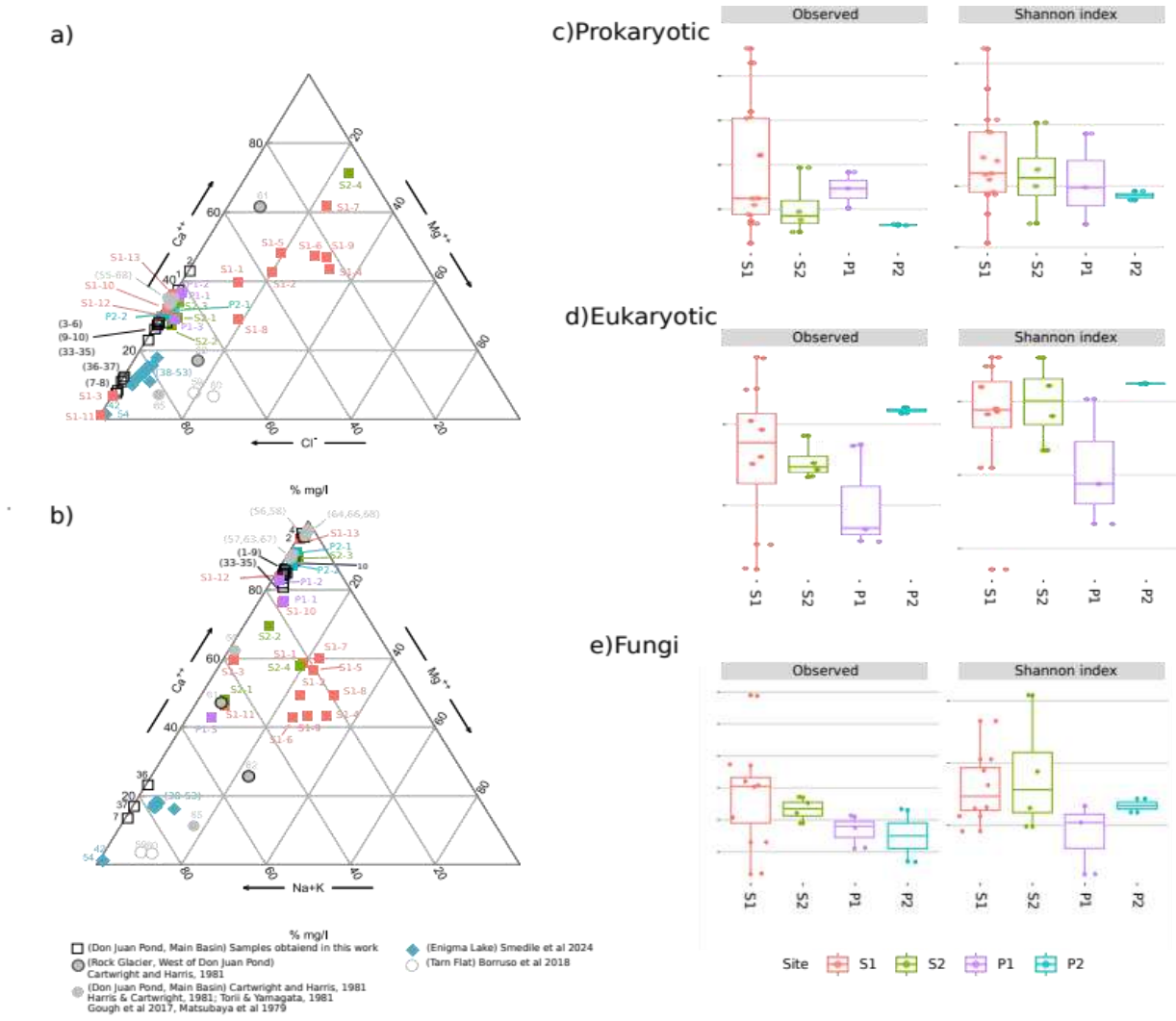


Figure 3. Hydrochemical composition and microbial alpha diversity across the DJP system. (a-b) Ternary diagram showing the relative proportions of major cations and and anion in water samples collected from the peripheral pond (P1, P2) and streams (S1, S2) during this study, compared with recent (this article) and historical datasets from main basin Don Juan Pond, the adjacent rock glacier, Tarn Flat, and Enigma Lake. (c–e) Alpha diversity metrics (Observed ASVs and Shannon index) derived from amplicon sequencing of the 16S rRNA gene (prokaryotes), the 18S rRNA gene (microeukaryotes), and the ITS region (fungi), respectively. Historical hydrochemical data were compiled from Harris and Cartwright (1981) [50], Torii and Yamagata (1981) [51], Matsubaya et al. (1979) [52], Gough et al. (2017) [53], Borruso et al. (2018) [54], and Smedile et al. (2024) [55].

Marked hydrochemical differences were also observed among the transient aquatic habitats. Stream S1, originating from meltwater draining the western rock glacier, displayed the widest chemical gradient along its course and the highest average chlorinity (4.45 mol kg^{-1}), reflecting progressive mixing between dilute meltwater and $CaCl_2$-rich brines. In contrast, stream S2 showed a much narrower chlorinity range (0.03–0.56 mol kg^{-1}), while the isolated pond P1 and the downstream pond P2 exhibited intermediate but distinct hydrochemical conditions, with average chlorinity values of 0.16 and 1.01 mol kg^{-1}, respectively (Additional file 1, table S1 and additional file 2).

3.3 Alpha diversity of microbial communities

Except for stream S3, all sampled habitats yielded DNA of sufficient quantity and quality for high-throughput metabarcoding. A total of 22 prokaryotic (16S rRNA), 17 microeukaryotic (18S rRNA), and 17 fungal (ITS2) libraries were successfully generated (Additional file 2).

Amplicon sequencing generated 871,806 high-quality prokaryotic reads, 1,987,436 microeukaryotic reads, and 665,637 fungal reads, corresponding to 15,892 16S ASVs, 2,644 18S ASVs, and 539 ITS2 OTUs, respectively. Across all datasets, the S1 stream system consistently supported the greatest microbial diversity within the DJP basin (Fig. 3c–e).

Prokaryotic communities exhibited the highest richness and diversity among the three datasets. Observed richness ranged from 447 ASVs (sample S1-9) to 1,324 ASVs (S1-7), while Shannon diversity varied between 5.04 and 6.62. Microeukaryotic communities were less diverse, with richness ranging from 21 to 283 ASVs and Shannon diversity from 0.72 to 3.60. Fungal assemblages displayed the lowest richness overall, ranging from 13 to 69 OTUs, with Shannon diversity values between 0.90 and 3.12. Because ITS2 sequences

were clustered at 97% similarity (Yang et al., 2018) whereas 16S and 18S datasets were analyzed at ASV resolution (99% similarity), fungal richness values should not be directly compared with those obtained for prokaryotes and microeukaryotes.

Interestingly, both the highest and lowest alpha-diversity values across all three datasets were predominantly associated with the S1 stream system. Rather than simply representing the most diverse habitat, S1 encompassed communities spanning a broad diversity spectrum, from highly diverse microbial mats to assemblages characterized by low richness and evenness.

Consistent with previous Antarctic metabarcoding studies, plastid- and mitochondria-derived 16S rRNA sequences were retained to capture the phototrophic component of the microbial communities [53,54].

3.4 Taxonomic composition of microbial communities

3.4.1 Prokaryotic communities

The taxonomic composition of prokaryotic communities varied markedly among the investigated habitats, although members of Pseudomonadota, Bacteroidota, and Bacillota consistently dominated the bacterial assemblages (Fig. 4). Pseudomonadota represented the most abundant phylum in the majority of samples, with Gammaproteobacteria and Alphaproteobacteria representing the predominant classes. Within these, Pseudomonadales, Hyphomicrobiales, Rhodobacterales, and Sphingomonadales were the most abundant orders.

Pseudomonadales dominated several stream-associated communities, accounting for more than 40–70% of the sequences in samples S1-6, S1-8 and S1-9. Hyphomicrobiales reached their highest relative abundance in S1-12 (approximately 40%) and represented 25–31% of pond communities, whereas Rhodobacterales were particularly abundant in the

P1 and S2 systems, where they accounted for 19–31% of the bacterial assemblages. Members of Bacteroidota, mainly represented by Flavobacteriales, formed the second major component of the communities and exceeded 35% of the sequences in pond samples, reaching approximately 63% in S2-4. Cytophagales and Chitinophagales were also recurrent, particularly within stream-associated microbial mats (Fig.4).

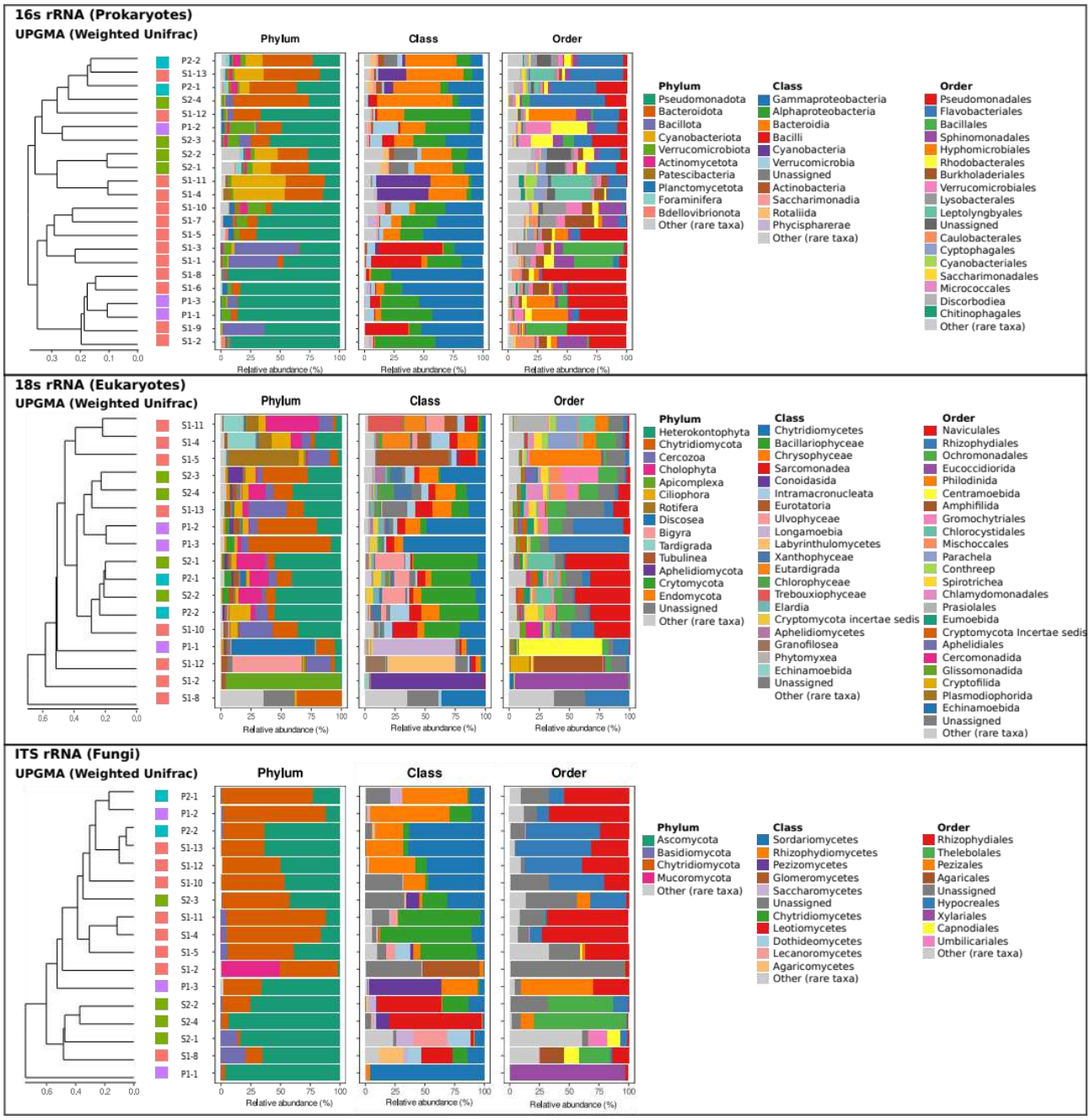


Figure 4. UPGMA clustering and taxonomic composition of microbial communities across the DJP basin based on prokaryotes, microeukaryotes, and fungi datasets.

Stacked bar plots show the relative abundance of dominant taxa at phylum, class, and order levels. Only the most abundant >1% present in at least 5 samples and prevalent taxa (at least two taxa for samples) are displayed, while remaining groups are merged as “Other (rare taxa)”.

Members of Bacillales dominated several samples from the S1 system, accounting for more than 50% of all sequences in S1-3 and exceeding 34% in S1-1 and S1-9, indicating pronounced spatial variability even within the same hydrological compartment. In addition, Cyanobacteriota, particularly Leptolyngbyales, formed localized phototrophic assemblages in S1-4, S1-10 and S1-13, where they represented 20–35% of the bacterial communities. Verrucomicrobiota were also consistently detected, reaching relative abundances above 20% in several P1, P2 and S2 samples.

Although members of the Patescibacteria, primarily represented by Saccharimonadales, were less abundant overall, they were present throughout the basin and reached their highest abundance in S1-10 (4.4%). Because plastid-derived 16S rRNA sequences were intentionally retained, the dataset also included chloroplast sequences affiliated with diatoms and green algae, providing complementary evidence for the presence of phototrophic microorganisms, which were later examined in more detail using the 18S rRNA dataset.

Unexpectedly, a subset proportion of plastid-associated 16S rRNA gene sequences was assigned to Foraminifera (Order Discorboidea) (Fig. 4). These sequences were detected in samples collected from all four hydrological compartments of the DJP basin and reached relative abundances of approximately 5% in samples P1-1 and S2-1. BLAST analysis of representative ASVs revealed 98.87% sequence identity and 100% query coverage with *Planoglabratella opercularis* isolate GO_m19-25 (GenBank accession KP792470), a shallow-water epibenthic foraminifer previously reported from marine coastal environments [57].

However, despite the use of universal eukaryotic primers, no foraminiferal sequences were recovered from the 18S rRNA dataset. Therefore, although the repeated detection of these plastid-associated signatures in several across multiple independent samples suggests that they are unlikely to represent a single analytical artefact, their taxonomic origin remains uncertain.

3.4.2 Microeukaryotic communities

Analysis of 18S rRNA dataset revealed complex microeukaryotic assemblages composed of phototrophic algae, heterotrophic protists, micro-metazoans and minor fungal component, the relative abundances of which varied markedly across the studied habitats (Fig. 4).

Phototrophic taxa constituted themajor fraction of the eukaryotic communities. Bacillariophyta (mainly Naviculales) dominated several samples, accounting for 53.8% and 45.4% of assigned sequences in S2-1 and S2-2, respectively, and more than 30% in P2 and S1-10. Chrysophyceae, primarily represented by Ochromonadales, were also widespread, accounting for 15–17% of sequences in S2-3, S2-4, P2-2 and S1-13. Green algae, primarily Ulvophyceae (Chlorocystidales), were particularly abundant in samples S2-1 and S2-2, where they accounted for 21.9% and 14.3% of the communities, respectively.

Heterotrophic protozoans were another important component of the eukaryotic assemblages. Cercozoa were consistently detected throughout the basin, with Cercomonadida, Glissomonadida, and Cryptofilida reaching their highest abundances in several S1 samples. Ciliates belonging to Spirotrichea and other Intramacronucleata were also recurrent, particularly in samples P2-2, S1-4, S2-3 and S1-13. Amoebozoa displayed

683 a more mosaic distribution, although Centramoebida dominated in sample P1-1, where
684 they accounted for approximately 69% of all assigned sequences.

685 A remarkable feature of the 18S dataset was the widespread occurrence of micro-
686 metazoans. Bdelloid rotifers (Philodinida) dominated samples S1-5, accounting for nearly
687 59% of all eukaryotic reads, while tardigrades (Parachela) accounted for 24% and 17% of
688 the communities in samples S1-4 and S1-11, respectively. Nematodes belonging to
689 Plectida and Rhabditida were also detected in several samples

690

691 **3.4.3 Fungal communities**

692 Fungal communities inferred from the ITS2 dataset were highly heterogeneous and were
693 overwhelmingly dominated by Ascomycota, followed by Chytridiomycota, although the
694 dominant taxa varied substantially across sampling sites (Fig. 4).

695 Hypocreales (Sordariomycetes) was the most abundant fungal order, dominating several
696 stream and pond communities, accounting for 48–64% of all reads in S1-10, S1-12, S1-13
697 and P2-2, and remaining abundant in S2-3 and P2-1. In contrast, Xylariales were almost
698 exclusively present in sample P1-1, where they represented approximately 96% of all
699 fungal sequences. Thelebolales (Leotiomycetes) dominated several stream-associated
700 habitats, accounting for 78% of all reads in S2-4 and exceeding 50% in sample S2-2.

701 Important additional components included Pezizomycetes (mainly represented by
702 Pezizales), which dominated sample P1-3 (61%), together with Dothideomycetes
703 (primarily Capnodiales) and Saccharomycetes, whose relative abundances varied across
704 the remaining habitats.

705 Early-diverging fungal lineages were also well represented. Members of Chytridiomycota,
706 particularly Rhizophydiales, were abundant in several habitats, accounting for 39% and
707 31% of the reads in S1-12 and S1-13, respectively, and dominated others, reaching 67%

in P1-2, and 55% in P2-1. Additional contributions from unidentified chytrids and Spizellomycetales indicate that early-diverging fungal lineages constitute a substantial component of the transient aquatic habitats surrounding Don Juan Pond.

Finally, Basidiomycota constituted only a minor component of the fungal communities. Nevertheless, representatives of Agaricales, Filobasidiales, and Kriegeriales were detected in several samples, occasionally reaching higher relative abundances.

3.4.4 Community clustering

Weighted UniFrac analyses were consistent with the observed taxonomic patterns (Fig. 4). Prokaryotic communities showed the clearest clustering according to the major hydrological components of the basin, with communities dominated by Bacillales, enriched in Pseudomonadales and Flavobacteriales, associated with cyanobacteria and forming distinct clades. In contrast, microeukaryotic and fungal communities displayed greater compositional variability among samples, reflecting the heterogeneous distribution of phototrophic algae, protozoa, micro-metazoans and fungal in transitional glacial meltwater habitats.

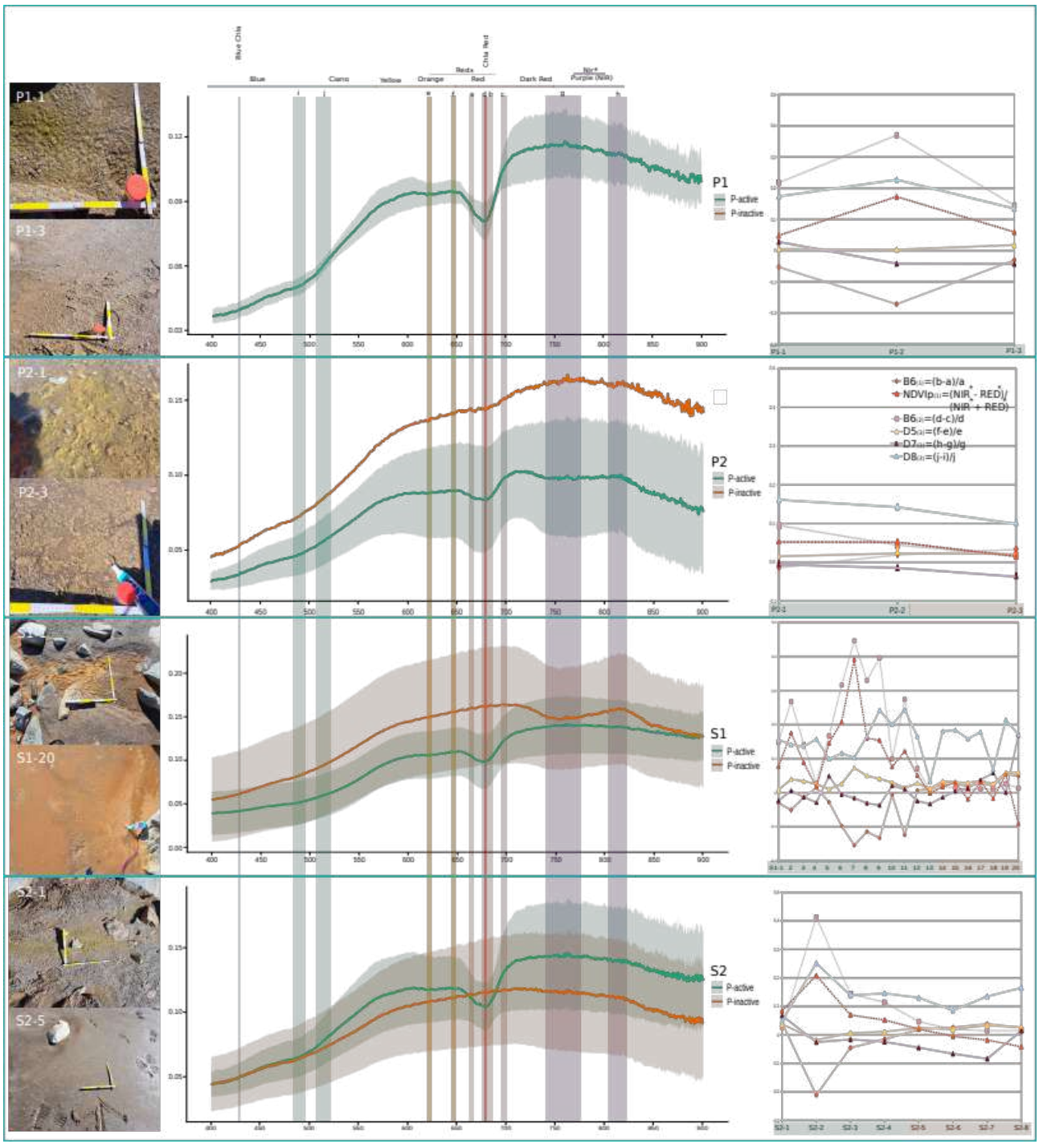
Taken together, the three metabarcoding datasets revealed a highly heterogeneous ecosystem in which closely spaced aquatic microhabitats supported markedly different prokaryotic, microeukaryotic and fungal communities despite sharing the same hydrological network.

3.5 Hyperspectral signatures of microbial mats

Hyperspectral reflectance analyses revealed distinct spectral signatures among microbial mats collected from the different transient aquatic habitats of the DJP basin (Fig. 5).

Although almost all samples exhibited the characteristic spectral features associated with photosynthetic communities, both the overall reflectance intensity and the shape of the spectra varied considerably among sites and between visually photosynthetically active (P-active) and degraded - inactive (P-inactive) microbial mats.

Reflectance spectra from all habitats displayed the typical absorption features in the blue (~450 nm) and red (~680 nm) regions, together with the progressive increase in reflectance across the green and near-infrared wavelengths that is characteristic of pigmented microbial communities. However, the magnitude of these features differed markedly among sites. Samples collected from stream S1 exhibited the highest spectral variability, consistent with the pronounced heterogeneity previously observed for both hydrochemical conditions and microbial diversity. In contrast, site P1 and S2 displayed relatively uniform spectral profiles, whereas sites P2 showed the greatest differences between P-active and P-inactive microbial mats, particularly in the red and near-infrared regions (Fig. 5).



747

748 **Figure 5**. **Reflectance spectra measured on surface sediments and microbial mats collected from**
749 **sampled hydrological compartments of the DJP basin (S1, S2 , P1 , and P2)**.
750 Representative photographs of photosynthetically active and degradated-inactive microbial mats and
751 sediment crusts are shown on the left. Colored vertical bands indicate the spectral regions used to calculate
752 pigment-related reflectance indices. The plots on the right summarize the variability of spectral indices
753 among samples within each hydrological compartment. Indices labeled as (1) were adopted from Levy et al.
754 (2020) [30], indices labeled as (2) were adapted from Di Mauro et al. (2020) [35], whereas indices labeled as

(3) were newly proposed in this study based on the analysis of the reflectance spectra collected from the DJP basin.

Spectral indices derived from the reflectance curves further highlighted habitat-specific differences. Chlorophyll absorption and near-infrared reflectance indices generally distinguished between living photosynthetically active, and degradated-inactive microbial communities, although the magnitude of these differences varied across habitats

The clearest separation was observed in P2, where several pigment-sensitive indices showed significant differences between P-active and P-inactive mats, whereas S1 exhibited greater within-site variability, reflecting the heterogeneous composition of microbial communities distributed along the meltwater drainage network. The P1 and S2 sites displayed intermediate and comparatively stable spectral responses.

3.6 Environmental and spectral drivers of microbial community assembly

The analyses of the environmental factors shaping microbial communities across the transient habitats of the DJP basin are illustrated in Fig. 6. While all three datasets exhibited significant environmental structuring, the relative importance of hydrochemical and spectral variables differed among prokaryotic, microeukaryotic and fungal communities (Additional file 2).

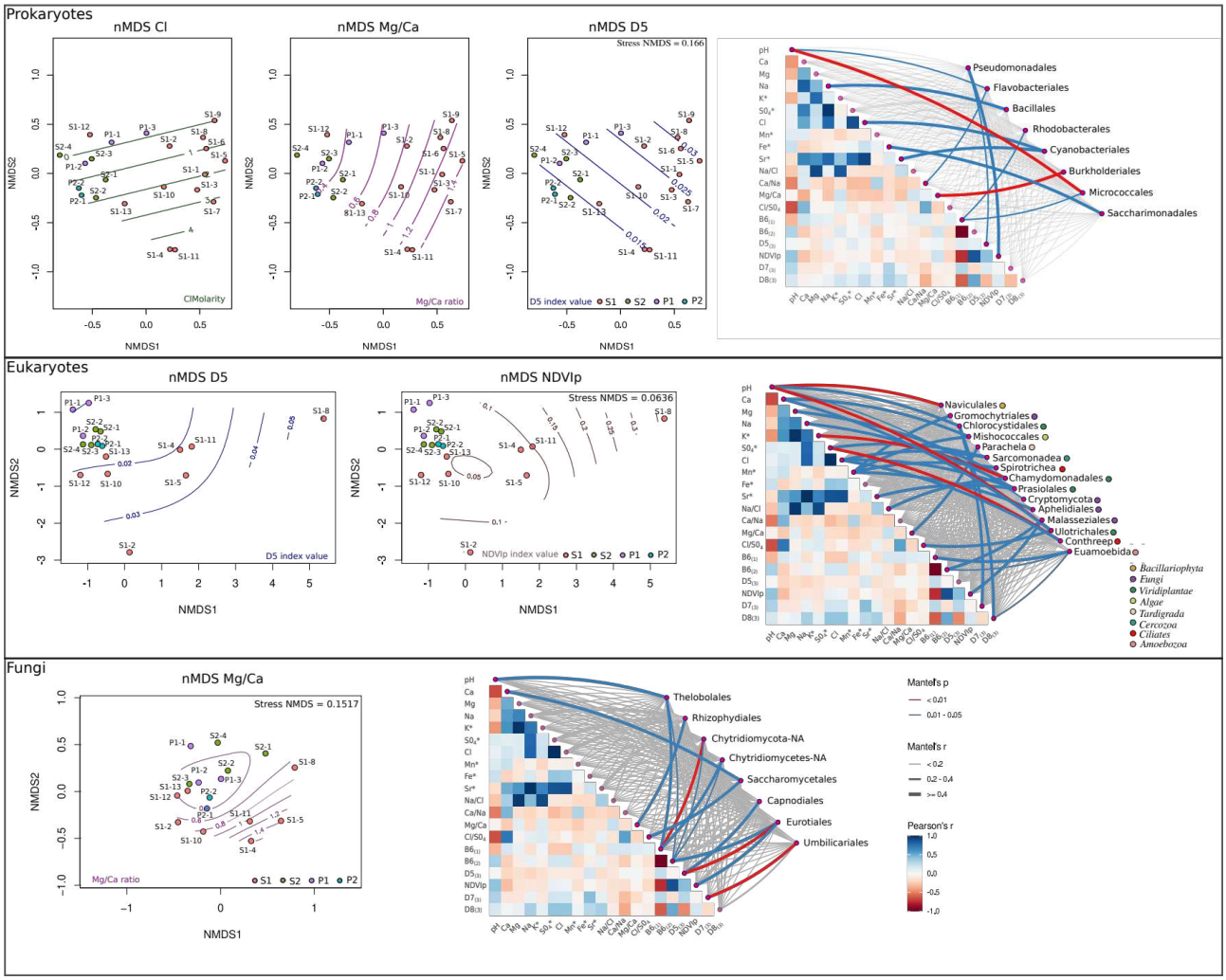
For prokaryotic communities, hydrological compartment identity (i.e., samples originating from the two stream systems, S1 and S2, and the two ponds, P1 and P2) explained a large and highly significant fraction of community variation ($r^2 = 0.485$, $p = 0.0002$ according to env-fit and $R = 0.2281$, p.value = 0.023 according to ANOSIM). Among continuous variables, env-fit evidenced Cl concentration ($r^2 = 0.265$, $p = 0.027$), and Mg/Ca ratio ($r^2 = 0.322$, $p = 0.020$) were significantly associated with community structure, while the D5 spectral index showed a weak relationship although did not reach statistical

significance (r^2 = 0.249, p = 0.062). Mantel tests further identified strong associations between Burkholderiales and Mg/Ca (r = 0.740, p = 0.001), Cyanobacteriales and Cl (r = 0.583, p = 0.016), Bacillales and Na (r = 0.480, p = 0.041), Saccharimonadales and Fe (r = 0.485, p = 0.042), and Pseudomonadales with both NDVIp (r = 0.447, p = 0.018) and D5 (r = 0.369, p = 0.021). Overall, these results indicate that prokaryotic assemblages were primarily structured by salinity-related geochemical gradients and water-body characteristics. The observed associations with spectral indices likely reflect the co-occurrence of bacterial populations with phototrophic microorganisms and pigmented microbial mats rather than direct responses of heterotrophic bacterial taxa to optical properties themselves.

Eukaryotic communities showed a different pattern. Hydrological compartment identity explained a smaller proportion of community variation (r^2 = 0.356) and was not statistically significant (p = 0.065) according to env-fit, similarly results were confirmed by ANOSIM test (R = 0.00913, p.value = 0.451). In contrast, the strongest continuous predictors were the hyperspectral indices D5 (r^2 = 0.429, p = 0.041) and NDVIp (r^2 = 0.421, p = 0.072), although only D5 reached statistical significance. These results suggest that eukaryotic community composition was more closely associated with photosynthetically active microbial mats than with bulk hydrochemistry. Mantel tests supported this interpretation, revealing multiple associations between eukaryotic groups and spectral or geochemical variables. Malasseziales correlated with B6(2), D5 and NDVIp, Euamoebida with B6(1), B6(2) and D8, Chlorocystidales with D7 and D8, and Parachela with Mg/Ca (r = 0.565, p = 0.031). Phototrophic groups such as Naviculales, Ulotrichales, Chlorocystidales, Chlamydomonadales and Prasiolales showed significant relationships with pH, Mg, Na, Na/Cl, Cl/SO4 and Sr, suggesting that algal and micro-metazoan assemblages were shaped by both spectral properties of active mats and local hydrochemical variability (Fig.6).

Fungal community composition was not significantly correlated with site identity (env-fit r^2 = 0.284, p = 0.151) and ANOSIM (P = 0.00623, p.value = 0.276), and only the Mg/Ca ratio showed a weak association with fungal ordination structure that did not reach statistical significance (r^2 = 0.306, p = 0.070). Mantel tests highlighted several significant relationships between fungal taxa and spectral indices, including Eurotiales with D5 (r = 0.716, p = 0.009), NDVIp (r = 0.833, p = 0.014), and B6(2) (r = 0.430, p = 0.021). Thelebolales were significantly associated with B6(1), B6(2) and pH, whereas Chytridiomycota-related lineages correlated with both B6(1) and B6(2). Saccharomycetales were correlated with Cl/SO4 and Ca, while Rhizophydiales were associated with the Mg/Ca (r = 0.473, p = 0.031). Overall, these results indicate that fungal assemblages were influenced more strongly by the occurrence of biologically active, pigment-rich microbial mats than broad hydrochemical gradients.

Taken together, the three metabarcoding datasets reveal a consistent ecological framework across the DJP basin. Hydrochemical gradients, particularly those associated with salinity and brine composition, exert the strongest influence on prokaryotic communities, while spectral properties associated with photosynthetic biomass become increasingly important for structuring microeukaryotic and fungal assemblages. Thus, the integration of hydrochemical and hyperspectral datasets provides additional valid information to explaining the succession of microbial communities in these temporary Antarctic habitats formed by mixing DJP brine with meltwater from nearby glaciers.



827

828 **Figure 6. Non-metric multidimensional scaling (nMDS) ordinations, environmental fitting analyses,**
829 **and Mantel correlations for prokaryotes, eukaryotic and fungal communities across the DJP**
830 **samples.**

831 Community composition was inferred from 16S rRNA (Prokaryotes), 18S rRNA (Eukaryotes) and ITS (Fungi)
832 datasets using Bray–Curtis dissimilarity matrices. Significant environmental gradients identified by envfit and
833 ordisurf analyses are shown as contour surfaces, highlighting the influence of chlorine concentration (Cl),
834 Mg/Ca ratio, D5 spectral index and NDVIp on community distribution. Samples are grouped according to
835 sampling areas (S1, S2, P1 and P2). The right panels show Mantel correlation networks linking the most
836 influential taxonomic orders identified by SIMPER analysis with environmental and hyperspectral variables. The
837 heatmaps represent Pearson correlation coefficients among environmental parameters, whereas connecting lines
838 indicate significant Mantel correlations. Line colour denotes Mantel significance level (red, $p < 0.01$; blue, $0.01 \leq p <$
839 0.05), while line thickness reflects Mantel's r value. Stress values are reported for each nMDS ordination. This

combined approach allowed the identification of both the main drivers shaping overall community structure and the specific environmental factors associated with the distribution of key microbial groups across the DJP basin.

3.7 Multi-domain ecological network reveals habitat-specific microbial consortia

The co-occurrence network analysis identified nine ecological modules across the microbial communities inhabiting the transient aquatic habitats of the DJP basin. However, more than 95% of all ASVs were concentrated within five major clusters (Clusters 1–5), indicating that the network was dominated by a limited number of highly structured ecological assemblages (Fig. 7). These modules differed markedly in taxonomic composition, network topology and habitat association, demonstrating that microbial communities were organized into distinct multi-domain consortia rather than randomly associated taxa.

Cluster 1 (244 ASVs) was primarily associated with pond P2 and stream S2 and consisted predominantly of Pseudomonadota, but also contained substantial numbers of Bacteroidota, Bacillota, Actinomycetota, and diverse other eukaryotic groups including Cercozoa, Heterokontophyta, and sequences assigned to Foraminifera. Similarly, Cluster 4 represented the largest module identified (295 ASVs) and displayed the highest eigenvector centrality, indicating its prominent position within the overall network (Additional file 2). In addition to prevailing Pseudomonadota and Bacteroidota, this cluster included numerous fungal and other eukaryotic taxa, particularly Chytridiomycota, Ascomycota, Cercozoa, Heterokontophyta, and Ciliophora, revealing extensive integration of bacterial, fungal and protistan lineages. Cluster 5 contained fewer ASVs (84) but exhibited the highest average degree, indicating exceptionally strong internal connectivity. This module was almost exclusively associated with pond P2 and likely represents a highly specialized microbial consortium adapted to the local physicochemical conditions of this habitat.

In contrast, stream-associated communities formed smaller and compositionally distinct modules. Cluster 2 (233 ASVs), predominantly associated with stream S1 and pond P1, exhibited the highest taxonomic diversity, containing numerous Pseudomonadota, Bacteroidota, Cyanobacteriota, Chlorophyta, Cercozoa, Ciliophora, Rotifera, and Tardigrada. The coexistence of phototrophic microorganisms, grazers and heterotrophic taxa suggests the presence of relatively mature microbial mat communities sustained by multiple trophic interactions. Cluster 3 (130 ASVs) was almost exclusively associated with stream S1 and P2 and was dominated by bacterial taxa, particularly Pseudomonadota, Bacteroidota, Actinomycetota, and Bacillota, whereas phototrophic and metazoan groups were comparatively less abundant, indicating a simpler and potentially more transient community structure.

Despite the clear habitat specificity of individual modules, all major clusters consistently included representatives of bacteria, fungi, protists, phototrophic algae and micro-metazoans. Within the obtained network, Pseudomonadota, Bacteroidota, Bacillota, Actinomycetota, Cyanobacteriota, and Verrucomicrobiota co-occurred with members of Heterokontophyta, Cercozoa, Ciliophora, Rotifera, Tardigrada, Chlorophyta, Ascomycota, Chytridiomycota, and Cryptomycota, indicating that microbial communities in the DJP basin function as integrated multi-domain ecological systems rather than independent bacterial, fungal or eukaryotic assemblages.

Overall, network analysis revealed that habitat type is the primary determinant of microbial associations within the basin. The two ponds harbored the largest and most interconnected ecological modules, while stream communities formed smaller, less interconnected assemblages, consistent with the greater hydrological stability of the ponds compared to the more dynamic conditions typical of moving meltwater.

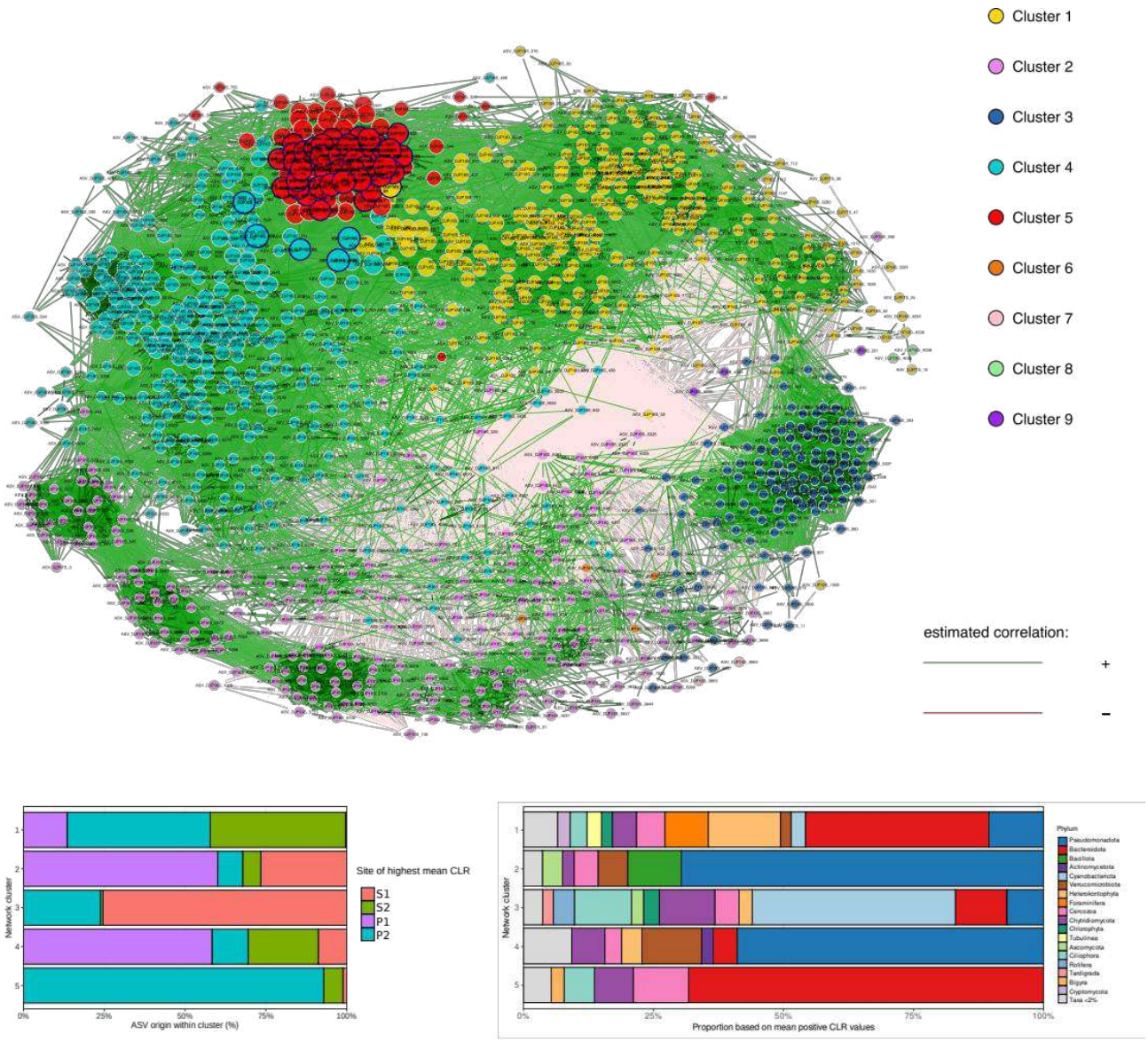


Figure 7. **Co-occurrence network of prokaryotic, eukaryotic and fungal ASVs from the DJP basin inferred from CLR-transformed abundance data**.

Nodes represent ASVs and edges represent significant positive (green) or negative (red) associations. ASVs are grouped into five major network modules (Clusters 1–5). Barplots summarize the taxonomic composition of each cluster based on mean positive CLR abundance and the relative contribution of ASVs originating from the four hydrological compartments (S1, S2, P1 and P2). The network highlights the existence of habitat-specific, multi-domain ecological assemblages linking bacterial, fungal and eukaryotic communities across the basin.

4. Discussion

4.1 Life at the edge of habitability: Don Juan Pond as a dynamic extreme ecosystem

Don Juan Pond is widely recognized as one of the most extreme aquatic environments on Earth. In addition to its exceptionally high $CaCl_2$ concentrations, extremely low water activity, intense osmotic and chaotropic stress, the basin is subjected to prolonged subzero temperatures, recurrent freeze–thaw cycles that periodically affect parts of the basin, episodic desiccation and intense solar / ultraviolet radiation, creating a truly polyextreme environment at the limits of habitability [12,23,24] . For these reasons, this basin has often been proposed as a terrestrial analogue for transient brine environments thought to have existed on early Mars [13] .

Previous investigations of DJP have primarily focused on the origin, hydrochemistry and stability of its $CaCl_2$-rich brines because of their astrobiological importance [13,18,48]. Although microbial mats and localized biological activity have occasionally been reported in peripheral ponds and ephemeral streams [14,23–25], the ecological relationships between hydrological variability, hydrochemistry and microbial community organization have remained largely unresolved. By integrating repeated field observations with hydrochemical analysis, hyperspectral reflectance, multi-domain DNA metabarcoding and ecological network reconstruction, our results provide a comprehensive ecological framework describing the occurrence, composition, and organization of microbial communities in a pond catchment.

Our results demonstrate that structured microbial communities are associated with transient meltwater-fed habitats surrounding the pond, whereas no evidence of comparable communities and/or traces of life was detected in the central $CaCl_2$ – saturated brine.

The comparison between the two Antarctic expeditions further emphasizes the importance of seasonal hydrological dynamics. During the 2021-2022 campaign, the basin

progressively evolved from a partially ice-covered lake to an evaporitic landscape dominated by extensive salt crusts, and no evidence of any active microbial communities was detected despite extensive sampling. Conversely, surveys conducted later in the austral summer during the 2022–2023 expedition revealed the development of meltwater-fed streams and shallow ponds originating from the western rock glacier, together with conspicuous microbial mats colonizing these newly formed aquatic habitats. Although the two campaigns also differed slightly in sampling period, with the second expedition extending into early January, the observations strongly suggest that seasonal meltwater availability is the primary factor controlling the formation and persistence of transient aquatic habitat capable of supporting structured microbial communities.

These findings indicate that Don Juan Pond should not be viewed as a single homogeneous hypersaline ecosystem. Instead, the basin functions as a dynamic hydrological landscape in which temporary freshwater influx locally reduces osmotic/chaotropic stress and creates heterogeneous microhabitats. Within these temporary refugia, microbial communities can nucleate, develop and interact before being progressively subjected again to evaporation, salt concentration and desiccation. The pronounced differences observed between streams and ponds further demonstrate that even small variations in hydrological connectivity can create distinct ecological niches within a relatively limited geographical area.

This interpretation also provides a broader perspective on habitability in polyextreme environments. The results indicate that the presence of liquid water alone is insufficient to explain the distribution of microbial life in the DJP basin. Rather, habitability emerges from the interaction between hydrological dynamics, hydrochemical evolution and environmental stability. Thus, seasonal meltwater therefore acts not simply as a water source, but as an ecological driver creating short-term habitability during which microbial communities can persist despite the surrounding polyextreme conditions. This dynamic

957 view of the DJP basin expands on previous conceptual models and highlights the
958 importance of temporary ecological refugia in defining the boundaries of life in similar
959 extraterrestrial environments making it one of the quintessential terrestrial analogues for
960 this type of study..

961

962 **4.2 Hydrochemical gradients drive microbial community assembly across transient**
963 **meltwater habitats**

964 Our multivariate analyses demonstrate that hydrochemical gradients represent the
965 principal environmental drivers shaping microbial community assembly across the
966 transient aquatic habitats of the DJP basin. Although all investigated habitats originated
967 from seasonal meltwater inputs, progressive evaporation and interaction with $CaCl_2$-rich
968 subsurface brines rapidly generated marked physicochemical differences among streams
969 and ponds. These hydrochemical gradients were consistently reflected in microbial
970 community composition, indicating that even subtle variations in water chemistry strongly
971 influence the establishment of microbial assemblages.

972 Among the measured environmental variables, chloride concentration, ionic strength and
973 the Mg/Ca ratio emerged as the strongest predictors of prokaryotic community structure.
974 These parameters are closely associated with the progressive evolution of $CaCl_2$-rich
975 brines and therefore represent effective proxies for the intensity of evaporative
976 concentration and water-rock interactions within the basin [18]. The strong association
977 between bacterial assemblages and these variables suggests that prokaryotic
978 communities respond rapidly to local geochemical conditions, with salinity acting as a
979 primary environmental driver selecting taxa capable of tolerating increasing
980 osmotic/chaotropic stress.

The Mg/Ca ratio was particularly informative, showing significant associations with both bacterial and fungal communities. Beyond representing simple differences in ionic composition, this ratio reflects the progressive geochemical evolution of meltwater during evaporation and mixing with concentrated subsurface brines. Similar hydrochemical gradients have previously been identified as major drivers of microbial community differentiation in Antarctic saline lakes and other hypersaline environments, where progressive changes in ionic composition often exert stronger ecological effects than salinity alone [18,52]. Our results suggest that a comparable process operates within the DJP basin, where local differences in brine evolution generate chemically distinct ecological niches over relatively short spatial scales.

Interestingly, fungal and microeukaryotic communities exhibited weaker responses to broad hydrochemical variables than prokaryotes. Instead, both fungal and microeukaryotic groups showed stronger associations with hyperspectral indices related to photosynthetic biomass, suggesting that habitat quality and biological productivity become increasingly important once suitable physicochemical conditions have been established. This pattern suggests a hierarchical process of community assembly in which hydrochemical gradients first determine the distribution of microbial habitats, while biological interactions and primary production subsequently contribute to structuring higher trophic levels.

The marked hydrochemical heterogeneity observed among streams and ponds further highlights the dynamic nature of the DJP basin. Although these habitats are separated by only a few tens of meters, differences in water residence time, evaporation intensity and connectivity with the rock glacier generate distinct physicochemical environments that support significantly different microbial communities. Rather than representing isolated aquatic systems, the transient habitats surrounding Don Juan Pond constitute a continuum of ecological niches linked by seasonal hydrological connectivity but differentiated by rapid local geochemical evolution.

Overall, these findings indicate that microbial community assembly within the DJP basin is primarily governed by the interaction between hydrological dynamics and hydrochemical evolution. Seasonal meltwater inputs create the physical habitat in which microbial life can develop, whereas subsequent evaporative concentration and changes in ionic composition determine which microbial taxa persist within each habitat. This conceptual framework provides a mechanistic explanation for the strong spatial organization observed across all three metabarcoding datasets and explains why neighboring streams and ponds despite their close geographical location, harbor markedly different microbial assemblages .

4.3 Hyperspectral reflectance as an indicator of microbial ecosystem function

Hyperspectral reflectance analyses provided an independent and non-destructive assessment of biological activity across the transient habitats of the DJP basin. Previous studies have demonstrated the potential of hyperspectral techniques for detecting biological soil crusts and microbial mats in Antarctic environments through the identification of pigment-specific absorption features [30,56,57]. Our results extend these observations by showing that hyperspectral signatures not only discriminate biologically active microbial mats from surrounding sediments, but also reflect broader patterns of microbial community organization.

Visible microbial mats consistently exhibited pronounced chlorophyll absorption around 680 nm together with elevated values of pigment-sensitive indices such as NDVIp, D5 and B6, whereas inactive sediments displayed relatively flat spectra and lower index values. The close correspondence between hyperspectral signatures, successful DNA recovery and PCR amplification strongly suggests that spectral measurements provide a reliable proxy for identifying biologically active habitats within this extremely heterogeneous environment. This capability is particularly valuable in Antarctic ecosystems, where biological colonization is often spatially patchy and biomass is extremely low.

An important observation emerging from this study is that spectral indices were associated not only with phototrophic microorganisms but also with the composition of bacterial, fungal and microeukaryotic communities. Several bacterial orders, including Pseudomonadota, as well as dominant fungal groups such as Eurotiales and Thelebolales, showed significant relationships with pigment-sensitive spectral indices. Likewise, numerous microeukaryotic taxa, including algae, amoebae and micro-metazoans, were associated with variations in reflectance properties. These findings indicate that hyperspectral signals capture the ecological state of the microbial mat as an integrated ecosystem, reflecting a measure of community, rather than simply detecting chlorophyll abundance.

This broader ecological interpretation is consistent with the highly integrated organization of Antarctic microbial mats. Photosynthetic microorganisms constitute the primary producers within these systems, creating structural complexity and providing organic substrates that support heterotrophic bacteria, fungi and microbial grazers. Consequently, changes in pigment composition detected through hyperspectral analyses are expected to propagate throughout the entire community, indirectly reflecting shifts in trophic structure, microbial interactions and ecosystem functioning.

Thus, combining hyperspectral imaging with DNA metabarcoding represents a particularly powerful approach for investigating microbial ecosystems in extreme environments. While metabarcoding provides high-resolution taxonomic information, hyperspectral analyses allow rapid identification of biologically active habitats without disturbing fragile ecosystems. Together, these complementary techniques enable efficient characterization of microbial diversity while substantially improving field-scale ecological surveys.

While the spatial resolution of current satellite imaging spectroscopy missions such as PRISMA and EnMAP [56,58] is too low (30m) for detecting mats from space, the

application of these methods to larger areas can be done exploiting drones equipped with Visible and Near-InfraRed (VNIR) cameras.

From an astrobiological perspective, these observations further highlight the value of hyperspectral approaches for the exploration of extreme extraterrestrial analogue environments. The ability to remotely identify localized, biologically active meltwater habitats within otherwise largely uninhabitable landscapes could significantly improve future biosignature detection strategies, both in polar deserts and in the exploration of transient saline environments on Mars or other planetary bodies.

4.4 Distinct ecological strategies underpin microbial community assembly in transient Antarctic habitats

The multi-domain metabarcoding approach revealed that the microbial communities inhabiting ephemeral meltwater habitats of the DJP basin are composed of organisms displaying markedly different ecological strategies for surviving under polyextreme conditions. Rather than representing a random assemblage of extremophiles, these communities comprise microbial groups characterized by distinct physiological adaptations, life-history strategies, and trophic roles, which collectively contribute to the formation of functional microbial ecosystems.

Among prokaryotes, the dominance of Pseudomonadota, Bacteroidota, Actinomycetota and Bacillota is consistent with previous observations from Antarctic lakes, saline soils and other cryospheric environments [52,59,60]. Many representatives of these phyla possess physiological traits that enhance survival under conditions of repeated freeze–thaw cycles, osmotic stress and prolonged nutrient deprivation, including the production of compatible solutes, extracellular polymeric substances, cold-active enzymes and metabolically flexible lifestyles.

A particularly striking example was provided by Flavobacteriales, whose ASVs showed up to 99.1% sequence similarity with *Gillisia xinjiangensis,* a moderately halophilic species originally isolated from the hypersaline Achikkul Lake in northwestern China [61] . These ASVs reached remarkably high relative abundances, exceeding 60% of the bacterial community in sample S2-4 and more than 30% in several additional samples characterized by elevated chlorinity. Together with the detection of other taxa closely related to previously described halotolerant microorganisms [61], these observations indicate that salinity-related environmental gradients exert strong ecological filtering on the bacterial community composition in the temporary habitats of the DJP basin.

An intriguing feature of the DJP bacterial community was the repeated detection of lineages classified as Minisyncoccota (Patescibacteria), a major lineage within the Candidate Phyla Radiation (CPR), particularly members of the order Saccharimonadales. These microorganisms, with limited autonomous metabolic capabilities, possess highly reduced genomes and are thought to rely on close metabolic associations with other bacteria and archaea, functioning as episymbionts attached to the cell walls of their hosts [62,63]. Their occurrence within the DJP microbial mats, together with their recent detection in other Antarctic polyextreme environments, including subglacial Lake Enigma [53] and the hypersaline subsurface brine system of the Boulder Clay area [60], suggests that ecological interactions and metabolic interdependencies may represent important mechanisms for their persistence under extreme conditions, where resource availability is both spatially heterogeneous and temporally constrained.

In contrast, microeukaryotic communities were dominated by organisms whose survival apparently depended less on physiological tolerance to hypersalinity than on remarkable resilience to repeated environmental fluctuations. Phototrophic groups, including chlorophytes, diatoms and other microalgae, likely serve as primary producers supporting the development of microbial mat during periods of active meltwater flow. Their

coexistence with heterotrophic protists, amoebozoans, ciliates and small metazoans, including rotifers, nematodes and tardigrades, indicates the establishment of relatively complex food webs despite extreme environmental setting. Many of these organisms are capable of entering dormant or cryptobiotic states during desiccation and freezing, allowing for rapid recolonization upon restoration of favourable hydrological conditions [64–66]. It should be emphasized that environmental DNA does not directly distinguish between metabolically active, dormant or recently deceased organisms. Therefore, the detection of eukaryotic taxa should be interpreted as evidence of their persistence in the system rather than as irrefutable proof of active growth in some of the most extreme conditions on our planet. Nevertheless, their repeated occurrence in various hydrological compartments strongly suggests that these organisms represent a genuine component of the DJP ecosystem.

The fungal communities revealed an equally diverse range of ecological strategies. Orders such as Thelebolales, Hypocreales and Xylariales dominated different habitats, reflecting the broad functional diversity of Antarctic fungi [67]. Members of Thelebolales are frequently reported from polar soils, microbial mats and ornithogenic environments, where they contribute to organic matter decomposition under repeated freeze–thaw cycles and prolonged cold conditions [68]. Many members of Hypocreales are versatile saprotrophs and opportunistic colonizers capable of rapidly exploiting transient nutrient availability, whereas Xylariales include fungi capable of degrading complex organic substrates and are known for their persistence under nutrient-limited conditions [68]. The high abundance of Chytridiomycota, particularly Rhizophydiales, is consistent with the ecology of these early-diverging fungi, which are typically associated with aquatic or periodically wet environments. Similar patterns have previously been reported from soils adjacent to ephemeral streams and ponds in the Antarctic Dry Valleys [69,70], supporting the importance of seasonal meltwater availability in structuring fungal communities,and

suggests close ecological associations with phototrophic microorganisms. The coexistence of these fungal groups suggests that fungal-mediated decomposition and organic matter recycling may represent important ecosystem processes even within these short-lived aquatic habitats [71].

Collectivelly, these observations indicate that microbial community assembly in the DJP basin reflects the convergence of multiple adaptive strategies rather than a single extremophile survival mechanism. Whereas many bacterial taxa appear to be physiologically adapted to persistent osmotic, chaotropic and thermal stress, numerous eukaryotes and fungi likely exploit the transient nature of these habitats through dormancy, rapid recolonization and flexible life-history strategies. Therefore, the exceptional biodiversity observed in DJP meltwater-brine habitats is best interpreted as the outcome of complementary ecological adaptations operating across multiple domains of life, allowing complex microbial ecosystems to develop during relatively short periods of favorable environmental conditions.

4.5 Unexpected biodiversity and possible dispersal pathways

One of the most unexpected findings of this study was the remarkable taxonomic diversity observed in the temporary microbial habitats surrounding Don Juan Pond. In addition to the expected assemblages of bacteria, cyanobacteria, microalgae and fungi commonly reported from Antarctic freshwater and terrestrial ecosystems, DNA metabarcoding revealed the presence of numerous protists and micro-metazoans, including several taxa that have rarely been documented in the McMurdo Dry Valleys. These observations suggest that the transient meltwater-brine habitats surrounding DJP support considerably more complex microbial ecosystems than previously thought.

Another unexpected discovery was the detection of plastid-associated sequences assigned to the foraminiferal order Discorboidea. Manual inspection of the corresponding ASVs revealed up to 98.9% sequence similarity and complete coverage with *Planoglabratella opercularis*, a cosmopolitan shallow-water epibenthic foraminifer [55]. Although fossil foraminiferal assemblages have previously been reported from Dry Valley sediments associated with past marine incursions [72–74] , and modern living foraminiferal communities are well known from the adjacent McMurdo Sound region [75,76], the detection of contemporary foraminiferal signatures in microbial mat of the land-locked Don Juan Pond basin is unexpected. If confirmed, this observation would expand the known ecological distribution of Antarctic foraminifera and suggest either the persistence of previously unrecognized inland populations or the existence of dispersal-mechanisms, likely aeolian, linking coastal and continental Antarctic habitats. Notably, no foraminiferal sequences were recovered from the 18S rRNA dataset, highlighting the need for independent confirmation through targeted molecular approaches and direct microscopic observations before definitive ecological conclusions can be drawn.

Several mechanisms could explain the occurrence of typical marine taxa within the DJP basin. Long range aeolian transport has previously been suggested as an important mechanism for microbial dispersal across Antarctica, allowing alive cells, spores and dormant forms to be transported over hundreds or even thousands of kilometers [77,78]. Alternatively, some propagules may originate from historical marine incursions associated with past glacial or lacustrine phases of the Wright Valley and, subsequently persist in sediments before becoming incorporated into newly developing microbial mats. Episodic transport by birds or human activities cannot be completely ruled-out, although these mechanisms are likely of minor importance in such a remote environment.

The discovery of unexpected eukaryotic lineages also highlights both the strengths and limitations of approaches based on environmental DNA analysis. High-throughput

metabarcoding significantly enhances our ability to deal with rare or low-abundance taxa that would likely escape detection by conventional microscopic observations [79]. However, this analysis alone is insufficient to prove that all detected organisms are metabolically active or permanently present in the ecosystem [80]. Some taxa may be present as dormant cysts, resting spores or their extracellular DNA may be preserved in sediments. Future studies integrating metatranscriptomics, cultivation-based approaches, fluorescence microscopy and fluorescence in situ hybridization (FISH) will therefore be essential to determine which members of these communities are actively contributing to ecosystem functioning.

4.4 Multi-domain ecological interactions revealed by network analysis

Although environmental gradients explained a significant portion of community variation, network analysis revealed an additional level of ecological organization in the DJP basin. The identified modules were composed not only of bacteria, fungi or microeukaryotes but also contained diverse assemblages of organisms belonging to all three domains, suggesting the existence of integrated ecological consortia.

The largest modules were predominantly associated with the peripheral ponds P1 and P2, where active microbial mats were most extensively developed. These clusters combined bacterial groups such as Pseudomonadota, Bacteroidota and Bacillota with phototrophic eukaryotes, fungal decomposers, protistan and micro-metazoans grazers. Such organization is consistent with structured trophic networks involving primary production, decomposition, nutrient recycling and microbial grazing.

The CLR-transformed abundances and connectivity metrics were particularly informative. Modules characterized by elevated mean CLR values and high numbers of ASVs constituents likely represent dominant ecological assemblages consistently enriched relative to the average community composition. Conversely, modules displaying

exceptionally high degree values despite lower richness suggest tightly interconnected consortia occupying specialized ecological niches. Cluster 5 is a striking example of this pattern, exhibiting relatively low species richness but the highest connectivity values and being strongly associated with the biologically active P2 pond.

The predominance of positive correlations throughout the network further suggests that cooperative interactions, metabolic complementarity and habitat sharing may play a major role in sustaining biodiversity under extreme environmental conditions. These findings indicate that microbial mats in DJP function as integrated multi-domain ecosystems rather than as collections of independent microbial populations.

4.6 Don Juan Pond and other athalassohaline hypersaline systems: contrasting models of life at the limits of habitability

The comparison between Don Juan Pond and other athalassohaline hypersaline environments provides an important framework for understanding how microbial life responds to physicochemical extremes. Among these systems, the magnesium-saturated (DHABs) of the Eastern Mediterranean represent one of the best-studied- models of long-term microbial adaptation to extreme ionic compositions and exceptionally high salinity. Unlike thalassohaline hypersaline systems, whose chemistry largely reflects concentrated seawater, DHABs are dominated by $MgCl_2$-rich brines, that impose intense chaotropic stress in addition to extremely low water activity. But while these basins themselves are lifeless, despite these severe physicochemical constraints, at the interface with seawater they support metabolically active microbial communities that have evolved in remarkably stable environmental conditions over geological time scales [7–11].

In other words, microbial life in these basins is unevenly distributed throughout the brine column. Biological activity is exclusively limited to areas of the salinity gradient where

seawater mixes with magnesium-rich brine and water activity and chaotropicity remain compatible with cellular functions, while the most concentrated brines of the basin itself exceed currently recognized physicochemical limits for life [8,9]. Thus, even in these persistently hypersaline systems, microbial communities occupy a relatively narrow range of physicochemical habitability, that is, in the interphase between the seawater column overlying the lake and the brine lake itself. Thus, there is a certain similarity between the presence of marginal life near (DJP) or above (DHAB) the dead brine.

Indeed, our results indicate that a comparable threshold also exists in the DJP basin, although under fundamentally different environmental setting. None of the archaeal taxa or specialized bacterial lineages typically associated with Mediterranean $MgCl_2$-rich brines were detected in DJP. Instead, the DJP microbial communities were dominated by bacterial, fungal and other eukaryotic taxa commonly reported from Antarctic terrestrial, freshwater and cryospheric environments. Biological activity was confined exclusively to peripheral streams and shallow ponds formed by seasonal meltwater inflow, while no evidence of active microbial communities was detected in the permanent central $CaCl_2$-rich brine. These observations indicate that the highly concentrated brine of DJP lies beyond the microbial habitability window, and its temporary dilution by glacial meltwater periodically restores physicochemical conditions compatible with microbial growth.

The contrasting ecology of these athalassohaline systems highlights the importance of environmental stability as primary determinant in formation of microbial communities. In Mediterranean DHABs, long-term physicochemical stability facilitated the evolution of highly specialized extremophilic communities capable of thriving near the edges of life imposed by $MgCl_2$-rich brines. In contrast, the DJP basin is constantly subject to hydrological disturbance caused by seasonal melting, evaporation and freeze–thaw cycles. Rather than fostering the formation of permanent extremophilic communities, these dynamics create short-lived habitats that are repeatedly colonized by microorganisms

combining physiological adaptation, dormancy, rapid recolonization, metabolic versatility and cooperative ecological interactions. Thus, community survival in DJP habitats depends not so much on long-term specialization as on the repeated reorganization of microbial ecosystems whenever suitable environmental conditions reappear.

Our findings also have important implications for astrobiology. They suggest that the mere presence of liquid brines is not, by itself, sufficient evidence of habitability. Instead, the persistence of microbial ecosystems likely depends on the existence of physicochemical windows in which water activity, chaotropicity, ionic composition and environmental stability remain compatible with sustained biological activity. Consequently, short-lived water bodies formed by episodic melting and/or subsurface hydrological processes may represent more promising targets for biosignature detection than permanently concentrated hypersaline reservoirs approaching, or even exceeding, the physicochemical limits of life.

Overall, our study demonstrates that Don Juan Pond should be viewed not simply as one of the most inhospitable ecosystems on Earth, but rather as a dynamic ecological landscape in which seasonal hydrological processes, albeit very rare and infrequently, create ephemeral windows of habitability at its peripheral margins enclosing a treasure chest of biodiversity and with multiple levels in the food chain. By integrating hydrochemistry, hyperspectral reflectance, multi-domain metabarcoding and ecological network analyses, we demonstrated that these temporary habitats sustain unexpectedly diverse and interconnected microbial communities whose organization is governed by the interplay of hydrology, geochemistry and ecological resilience. Taken together, these findings support a dynamic perspective on habitability in which the persistence of life depends not only on the availability of liquid water, but also on the repeated creation of environmental conditions that permit microbial communities to form, function and persist.

5. Conclusions

This study represents the first comprehensive ecological characterization of the transient microbial ecosystems surrounding Don Juan Pond by integrating hydrochemical analyses, hyperspectral reflectance spectroscopy, multi-domain DNA metabarcoding and ecological network reconstruction. Together, these complementary approaches demonstrated that biological activity in the basin is governed by the interplay of hydrological dynamics, geochemical evolution and ecological processes rather than by salinity alone

Our results demonstrate that the permanent $CaCl_2$-rich central brine remains largely inhospitable for microbial life, while seasonal meltwater inflows from the adjacent rock glacier create short-lived ecological niche supporting unexpectedly diverse and interconnected microbial communities. These habitats host bacteria, fungi, protists, microalgae and micro-metazoans organized into complex multi-domain assemblages whose composition varies along local hydrochemical gradients.

By combining molecular and hyperspectral approaches, we further demonstated that pigment-sensitive spectral indices provide reliable indicators of photosynthetically active microbial mats and enable the identification of ecosystem-level patterns extending far beyond phototrophic organisms only. This highlights the potential of hyperspectral techniques as rapid, non-invasive tools for detecting and monitoring microbial ecosystems in extreme environments.

The discovery of highly diverse microbial assemblages, including unexpected eukaryotic lineages and CPR bacteria, suggests that transient Antarctic habitats may function as ecological refugia and repositories of microbial biodiversity, where organisms employing distinct adaptive strategies coexist during relatively short periods of favorable environmental conditions. These results indicate that ecological resilience, metabolic

flexibility and community interactions likely play a more important role than previously thought in sustaining life under multiple extreme conditions.

More broadly, our study suggests that DJP basin represents a fundamentally different model of habitability compared to permanently stable hypersaline athalassohaline systems such as the Eastern Mediterranean DHABs. While long-term stable brines facilitate evolutionary specialization, the transient habitats surrounding DJP appear to promote survival through repeated ecological reassembly driven by seasonal hydrological processes. This distinction emphasizes that environmental stability may be as important as physicochemical extremes in determining the long-term persistence of microbial ecosystems.

Future studies integrating seasonal monitoring, cultivation, microscopy, metatranscriptomics, metaproteomics and metabolomics will be essential for distinguishing active populations from dormant or transient propagules and for unravelling the functional interactions that sustain these communities. Ultimately, the conceptual framework proposed here extends beyond Antarctica, providing new insights into the environement limits of life on Earth and facilitating the identification of potential habitable environments and biosignatures in hypersaline systems on Mars and other planetary bodies beyond the Earth.

Ethics approval and consent to participate

Not applicable

Consent for publication

Not applicable

Clinical trial number

Not applicable

Availability of data and materials

The sequencing datasets generated during this study are publicly available in the European Nucleotide Archive (ENA)/NCBI under BioProject accession number **PRJNA1495185**. Sample metadata, environmental parameters, and all additional datasets supporting the findings of this study are provided in **Additional file 1** and **Additional file 2**. The custom R scripts used for data processing, statistical analyses, and figure generation are publicly available in the project GitHub repository (https://github.com/GiISP/Don-Juan-Pond), together with the associated metadata required to reproduce the analyses.

Additional files provided with the manuscript:

Additional file 1

title:

Additional file 1, Orthomosaic of DJP and chemical data of sampled points..docx.

Description of Additional file 1

The Additional file 1 includes Figure S1, showing the orthomosaic of the Don Juan Pond basin and the location of the sampling sites, and Table S1, reporting the hydrochemical characteristics of the investigated samples together with comparative historical data from Antarctic saline environments.

Additional file 2.

title:

Additional file 2, Full account of metadata and statistical analysis.xlsx

Description of Additional file 2:

Additional file 2 is an excel file compiling the environmental and microbiological data used in the study, including microbial diversity and taxonomic profiles, spectral reflectance indices, hydrochemical variables, and the outputs of the main multivariate and statistical analyses. The file also includes CLR-transformed community data and cluster-based summaries used for the integrated analysis of the Don Juan Pond samples.

Abbreviations

DJP: Don Juan Pond; OTU: operational taxonomic unit; AVS: Amplicon sequence variants; PCR: polymerase chain reaction.

Competing interests

The authors declare that they have no competing interests

Funding

This study was funded by the National Antarctic Research Program (Programma Nazionale di Ricerche in Antartide or PNRA) (grant no PNRA18_00221 - E administered by the Italian Ministry of Education and Research. This study was also supported partially by grants from the FuturEnzyme Project (contract 101000327), funded by the European Union's Horizon 2020 Research Program and by grant from the HaloVita Project (PRIN 20225ERBRS) funded by MIUR Progetti di Ricerca di Rilevante Interesse Nazionale.

Authors' contributions

F.S., G.L.S., M.M.Y., and B.D.M. conceived and designed the study. F.S., V.L.C., M.A., B.D.M., L.Z., and M.M.Y. conducted field sampling during the Antarctic expeditions. V.L.C., G.L.S., L.M., F.C., F.Ca., V.A.L., C.P., T.C. and G.T. carried out the laboratory analyses. F.S., G.L.S., F.C., F.Ca., N.P., M.G., V.A.L., C.P., T.C. G.T., and B.D.M. performed the bioinformatic and statistical analyses. F.S., L.Z. and M.M.Y. drafted the manuscript. F.S., G.L.S., F.Ca., L.Z., and M.M.Y. interpreted the data. All authors critically revised the manuscript, approved the final version of the manuscript, and agree to be accountable for all aspects of the work.

Acknowledgements

The authors are thankful to the National Antarctic Research Program of Italy (PNRA),
The authors also thank the helicopter pilots for having supported the field logistics, the two UAV pilots from the National Agency for New Technologies, Energy and Sustainable Economic Development (ENEA) for their surveys and Dr. G. Bianchi Fasani (ENEA) for having supported the field campaign as station logistic leader

References

1. McKay CP. Requirements and limits for life in the context of exoplanets. *Proc Natl Acad Sci U S A*. 2014;111(35):12628-12633. doi:10.1073/pnas.1304212111

2. Méndez A, Rivera-Valentín EG, Schulze-Makuch D, et al. Habitability Models for Astrobiology. *Astrobiology*. 2021;21(8):1017-1027. doi:10.1089/ast.2020.2342

3. Merino N, Aronson HS, Bojanova DP, et al. Living at the Extremes: Extremophiles and the Limits of Life in a Planetary Context. *Front Microbiol*. 2019;10. doi:10.3389/fmicb.2019.00780

4. Yamagishi A, Kawaguchi Y, Hashimoto H, et al. Environmental Data and Survival Data of Deinococcus aetherius from the Exposure Facility of the Japan Experimental Module of the International Space Station Obtained by the Tanpopo Mission. *Astrobiology*. 2018;18(11):1369-1374. doi:10.1089/ast.2017.1751

5. Cottin H, Kotler JM, Bartik K, et al. Astrobiology and the Possibility of Life on Earth and Elsewhere…. *Space Sci Rev*. 2017;209(1):1-42. doi:10.1007/s11214-015-0196-1

6. Hand KP, Sotin C, Hayes A, Coustenis A. On the Habitability and Future Exploration of Ocean Worlds. *Space Sci Rev*. 2020;216(5):95. doi:10.1007/s11214-020-00713-7

7. La Cono V, Bortoluzzi G, Messina E, et al. The discovery of Lake Hephaestus, the youngest athalassohaline deep-sea formation on Earth. *Sci Rep*. 2019;9(1):1. doi:10.1038/s41598-018-38444-z

8. Yakimov MM, La Cono V, Spada GL, et al. Microbial community of the deep-sea brine Lake Kryos seawater–brine interface is active below the chaotropicity limit of life as revealed by recovery of mRNA. *Environ Microbiol*. 2015;17(2):2. doi:10.1111/1462-2920.12587

9. Hallsworth JE, Yakimov MM, Golyshin PN, et al. Limits of life in MgCl2-containing environments: chaotropicity defines the window. *Environ Microbiol*. 2007;9(3):801-813. doi:10.1111/j.1462-2920.2006.01212.x

10. Fisher LA, Pontefract A, M Som S, et al. Current state of athalassohaline deep-sea hypersaline anoxic basin research-recommendations for future work and relevance to astrobiology. *Environ Microbiol*. 2021;23(7):3360-3369. doi:10.1111/1462-2920.15414

11. Polonia A, Asioli A, Ferraro L, et al. Seismically triggered anoxia and brine spillover during the CE 365 Crete mega-earthquake in the eastern Mediterranean Sea. *Gondwana Res*. 2026;151:206-231. doi:10.1016/j.gr.2025.10.016

12. Samarkin VA, Madigan MT, Bowles MW, et al. Abiotic nitrous oxide emission from the hypersaline Don Juan Pond in Antarctica. *Nat Geosci*. 2010;3(5):5. doi:10.1038/ngeo847

13. Dickson JL, Head JW, Levy JS, Marchant DR. Don Juan Pond, Antarctica: Near-surface CaCl2-brine feeding Earth's most saline lake and implications for Mars. *Sci Rep*. 2013;3(1):1166. doi:10.1038/srep01166

14. Shaffer JMC, Giddings LA, Samples RM, Mikucki JA. Genomic and phenotypic characterization of a red-pigmented strain of Massilia frigida isolated from an Antarctic microbial mat. *Front Microbiol*. 2023;14. doi:10.3389/fmicb.2023.1156033

15. Meyer GH, Morrow MB, Wyss O, Berg TE, Littlepage JL. Antarctica: The Microbiology of an Unfrozen Saline Pond. *Science*. 1962;138(3545):3545. doi:10.1126/science.138.3545.1103

16. Harris HJH, Cartwright K, Torii T. Dynamic Chemical Equilibrium in a Polar Desert Pond: A Sensitive Index of Meteorological Cycles. *Science*. 1979;204(4390):301-303. doi:10.1126/science.204.4390.301

17. Doran PT, McKay CP, Clow GD, et al. Valley floor climate observations from the McMurdo dry valleys, Antarctica, 1986–2000. *J Geophys Res Atmospheres*. 2002;107(D24):ACL 13-1-ACL 13-12. doi:10.1029/2001JD002045

18. Toner JD, Catling DC, Sletten RS. The geochemistry of Don Juan Pond: Evidence for a deep groundwater flow system in Wright Valley, Antarctica. *Earth Planet Sci Lett*. 2017;474:190-197. doi:10.1016/j.epsl.2017.06.039

19. Anderson RC, Dohm JM, Buczkowski D, Wyrick DY. Early Noachian terrains: Vestiges of the early evolution of Mars. *Icarus*. 2022;387:115170. doi:10.1016/j.icarus.2022.115170

20. Foerder AB, Englert PAJ, Bishop JL, et al. Don Juan Basin, Antarctica: A chemically altering environment with martian analog potential. *Am Mineral*. 2024;109(4):682-700. doi:10.2138/am-2022-8779

21. Cartwright K, Harris HJH. Hydrogeology of the Dry Valley Region, Antarctica. In: *Dry Valley Drilling Project*. American Geophysical Union (AGU); 1981:193-214. doi:10.1029/AR033p0193

22. Winsor K, Swanger KM, Babcock EL, Dickson JL, Valletta RD, Schmidt DF. Origin, structure and geochemistry of a rock glacier near Don Juan Pond, Wright Valley, Antarctica. *Antarct Sci*. 2020;32(4):273-287. doi:10.1017/S0954102020000139

23. Siegel BZ, Mcmurty G, Siegel SM, Chen J, Larock P. Life in the calcium chloride environment of Don Juan Pond, Antarctica. *Nature*. 1979;280(5725):5725. doi:10.1038/280828a0

24. Siegel BZ, Siegel SM, Chen J, LaRock P. An extraterrestrial habitat on Earth: the algal mat of Don Juan [correction of Jaun] Pond. *Adv Space Res Off J Comm Space Res COSPAR*. 1983;3(8):8.

25. Shaffer JMC, Jarratt A, Boles BW, Mikucki JA. Draft genomes of three abundant bacterial isolates from hypersaline Don Juan Pond, Antarctica. *Microbiol Resour Announc*. 15(2):e00279-25. doi:10.1128/mra.00279-25

26. Klindworth A, Pruesse E, Schweer T, et al. Evaluation of general 16S ribosomal RNA gene PCR primers for classical and next-generation sequencing-based diversity studies. *Nucleic Acids Res*. 2013;41(1):1. doi:10.1093/nar/gks808

27. Chakraborty C, Doss CGP, Patra BC, Bandyopadhyay S. DNA barcoding to map the microbial communities: current advances and future directions. *Appl Microbiol Biotechnol*. 2014;98(8):3425-3436. doi:10.1007/s00253-014-5550-9

28. Chan Y, Van Nostrand JD, Zhou J, Pointing SB, Farrell RL. Functional ecology of an Antarctic Dry Valley. *Proc Natl Acad Sci U S A*. 2013;110(22):22. doi:10.1073/pnas.1300643110

29. Buelow HN, Winter AS, Van Horn DJ, et al. Microbial Community Responses to Increased Water and Organic Matter in the Arid Soils of the McMurdo Dry Valleys, Antarctica. *Front Microbiol*. 2016;7. doi:10.3389/fmicb.2016.01040

30. Levy J, Cary SC, Joy K, Lee CK. Detection and community-level identification of microbial mats in the McMurdo Dry Valleys using drone-based hyperspectral reflectance imaging. *Antarct Sci*. 2020;32(5):367-381. doi:10.1017/S0954102020000243

31. Jiang X, Van Horn DJ, Okie JG, et al. Limits to the three domains of life: lessons from community assembly along an Antarctic salinity gradient. *Extremophiles*. 2022;26(1):15. doi:10.1007/s00792-022-01262-3

32. Panigada C, Tagliabue G, Zaady E, et al. A new approach for biocrust and vegetation monitoring in drylands using multi-temporal Sentinel-2 images. *Prog Phys Geogr Earth Environ*. 2019;43(4):496-520. doi:10.1177/0309133319841903

33. Naethe P, De Sanctis A, Burkart A, et al. Towards a standardized, ground-based network of hyperspectral measurements: Combining time series from autonomous field spectrometers with Sentinel-2. *Remote Sens Environ*. 2024;303:114013. doi:10.1016/j.rse.2024.114013

34. Traversa G, Scipinotti R, Pierattini S, Fasani GB, Mauro BD. Cryoconite holes geomorphometry, spatial distribution and radiative impact over the Hells Gate Ice Shelf, East Antarctica. *Ann Glaciol*. Published online April 25, 2024:1-10. doi:10.1017/aog.2024.20

35. Di Mauro B, Garzonio R, Baccolo G, et al. Glacier algae foster ice-albedo feedback in the European Alps. *Sci Rep*. 2020;10(1):1. doi:10.1038/s41598-020-61762-0

36. Zhou J, Bruns MA, Tiedje JM. DNA recovery from soils of diverse composition. *Appl Environ Microbiol*. 1996;62(2):316-322. doi:10.1128/aem.62.2.316-322.1996

37. Amaral-Zettler LA, McCliment EA, Ducklow HW, Huse SM. Correction: A Method for Studying Protistan Diversity Using Massively Parallel Sequencing of V9 Hypervariable Regions of Small-Subunit Ribosomal RNA Genes. *PLOS ONE*. 2009;4(12):10.1371/annotation/50c43133. doi:10.1371/annotation/50c43133-0df5-4b8b-8975-8cc37d4f2f26

38. Caporaso JG, Lauber CL, Walters WA, et al. Ultra-high-throughput microbial community analysis on the Illumina HiSeq and MiSeq platforms. *ISME J*. 2012;6(8):8. doi:10.1038/ismej.2012.8

39. White T, Bruns T, Lee S, et al. Amplification and Direct Sequencing of Fungal Ribosomal RNA Genes for Phylogenetics. In: *Pcr Protocols: A Guide to Methods and Applications,*. Vol 31. 1990:315-322.

40. Callahan BJ, Sankaran K, Fukuyama JA, McMurdie PJ, Holmes SP. Bioconductor Workflow for Microbiome Data Analysis: from raw reads to community analyses. *F1000Research*. 2016;5:1492. doi:10.12688/f1000research.8986.2

41. Callahan BJ, McMurdie PJ, Rosen MJ, Han AW, Johnson AJA, Holmes SP. DADA2: High-resolution sample inference from Illumina amplicon data. *Nat Methods*. 2016;13(7):581-583. doi:10.1038/nmeth.3869

42. Rognes T, Flouri T, Nichols B, Quince C, Mahé F. VSEARCH: a versatile open source tool for metagenomics. *PeerJ*. 2016;4:e2584. doi:10.7717/peerj.2584

43. McMurdie PJ, Holmes S. phyloseq: An R Package for Reproducible Interactive Analysis and Graphics of Microbiome Census Data. *PLOS ONE*. 2013;8(4):e61217. doi:10.1371/journal.pone.0061217

44. Shetty SA, Lahti L. Microbiome data science. *J Biosci*. 2019;44(5):115.

45. Liu C, Cui Y, Li X, Yao M. microeco: an R package for data mining in microbial community ecology. *FEMS Microbiol Ecol*. 2021;97(2):fiaa255. doi:10.1093/femsec/fiaa255

46. Peschel S, Müller CL, von Mutius E, Boulesteix AL, Depner M. NetCoMi: network construction and comparison for microbiome data in R. *Brief Bioinform*. 2021;22(4):bbaa290. doi:10.1093/bib/bbaa290

47. Rasmussen TB, Noell SE, Herbold CW, et al. Geothermal ecosystems on Mt. Erebus, Antarctica, support diverse and taxonomically novel biota. *FEMS Microbiol Ecol*. 2024;100(11):fiae128. doi:10.1093/femsec/fiae128

48. Harris HJH, Cartwright K. Hydrology of the Don Juan Basin, Wright Valley, Antarctica. In: *Dry Valley Drilling Project*. American Geophysical Union (AGU); 1981:161-184. doi:10.1029/AR033p0161

49. Torii T, Murata S, Yamagata N. Geochemistry of the Dry Valley lakes. *J R Soc N Z*. 1981;11(4):387-399. doi:10.1080/03036758.1981.10423329

50. Matsubaya O, Sakai H, Torii T, Burton H, Kerry K. Antarctic saline lakes—stable isotopic ratios, chemical compositions and evolution. *Geochim Cosmochim Acta*. 1979;43(1):7-25. doi:10.1016/0016-7037(79)90042-5

51. Gough RV, Wong J, Dickson JL, et al. Brine formation via deliquescence by salts found near Don Juan Pond, Antarctica: Laboratory experiments and field observational results. *Earth Planet Sci Lett*. 2017;476:189-198. doi:10.1016/j.epsl.2017.08.003

52. Borruso L, Sannino C, Selbmann L, et al. A thin ice layer segregates two distinct fungal communities in Antarctic brines from Tarn Flat (Northern Victoria Land). *Sci Rep*. 2018;8(1):6582. doi:10.1038/s41598-018-25079-3

53. Smedile F, La Cono V, Urbini S, et al. The perennially ice-covered Lake Enigma, Antarctica supports unique microbial communities. *Commun Earth Environ*. 2024;5(1):1-17. doi:10.1038/s43247-024-01842-5

54. Hirose Y, Shiozaki T, Otani M, et al. Investigating Algal Communities in Lacustrine and Hydro-Terrestrial Environments of East Antarctica Using Deep Amplicon Sequencing. *Microorganisms*. 2020;8(4):4. doi:10.3390/microorganisms8040497

55. Tsuchiya M, Miyawaki S, Oguri K, et al. Acquisition, Maintenance, and Ecological Roles of Kleptoplasts in Planoglabratella opercularis (Foraminifera, Rhizaria). *Front Mar Sci*. 2020;7. doi:10.3389/fmars.2020.00585

56. Di Mauro B, Cogliati S, Bohn N, et al. Evaluation of PRISMA Products Over Snow in the Alps and Antarctica. *Earth Space Sci*. 2024;11(7):e2023EA003482. doi:10.1029/2023EA003482

57. Walshaw CV, Gray A, Fretwell PT, et al. A satellite-derived baseline of photosynthetic life across Antarctica. *Nat Geosci*. 2024;17(8):755-762. doi:10.1038/s41561-024-01492-4

58. Brell M, Reiners P, Guanter L, et al. Assessment of EnMAP data quality through global product validation activities. *Remote Sens Environ*. 2026;342:115459. doi:10.1016/j.rse.2026.115459

59. Michaud L, Caruso C, Mangano S, Interdonato F, Bruni V, Lo Giudice A. Predominance of Flavobacterium, Pseudomonas, and Polaromonas within the prokaryotic community of freshwater shallow lakes in the northern Victoria Land, East Antarctica. *FEMS Microbiol Ecol*. 2012;82:391-404. doi:10.1111/j.1574-6941.2012.01394.x

60. Papale M, Sannino C, Battistel D, et al. Revealing unexplored bacterial and fungal variability in interconnected Antarctic brines. *Curr Res Microb Sci*. 2026;10:100538. doi:10.1016/j.crmicr.2025.100538

61. Wang H hao, Zhang C, Chen Y qin, et al. Genomic characterization of *Gillisia xinjiangensis* sp. nov.: insights into nitrogen metabolism, stress adaptation, and application potential. *Syst Appl Microbiol*. 2025;48(5):126645. doi:10.1016/j.syapm.2025.126645

62. Brown CT, Hug LA, Thomas BC, et al. Unusual biology across a group comprising more than 15% of domain Bacteria. *Nature*. 2015;523(7559):7559. doi:10.1038/nature14486

63. Castelle CJ, Banfield JF. Major New Microbial Groups Expand Diversity and Alter our Understanding of the Tree of Life. *Cell*. 2018;172(6):6. doi:10.1016/j.cell.2018.02.016

64. Boothby TC, Tapia H, Brozena AH, et al. Tardigrades Use Intrinsically Disordered Proteins to Survive Desiccation. *Mol Cell*. 2017;65(6):975-984.e5. doi:10.1016/j.molcel.2017.02.018

65. Hespeels B, Fontaneto D, Cornet V, et al. Back to the roots, desiccation and radiation resistances are ancestral characters in bdelloid rotifers. *BMC Biol*. 2023;21(1):72. doi:10.1186/s12915-023-01554-w

66. Treonis AM, Wall DH. Soil nematodes and desiccation survival in the extreme arid environment of the antarctic dry valleys. *Integr Comp Biol*. 2005;45(5):741-750. doi:10.1093/icb/45.5.741

67. Márquez-Sanz R, Garrido-Benavent I, Durán J, de los Ríos A. The Establishment of a Terrestrial Macroalga Canopy Impacts Microbial Soil Communities in Antarctica. *Microb Ecol*. 2025;88(1):4. doi:10.1007/s00248-025-02501-8

68. Ogaki M, Vieira R, Juan M. L, Rosa C, Rosa L. Diversity and Ecology of Fungal Assemblages Present in Lakes of Antarctica. In: 2019:69-97. doi:10.1007/978-3-030-18367-7_4

69. Canini F, Geml J, Buzzini P, et al. Growth Forms and Functional Guilds Distribution of Soil Fungi in Coastal Versus Inland Sites of Victoria Land, Antarctica. *Biology*. 2021;10(4):320. doi:10.3390/biology10040320

70. Bridge PD, Newsham KK. Soil fungal community composition at Mars Oasis, a southern maritime Antarctic site, assessed by PCR amplification and cloning. *Fungal Ecol*. 2009;2(2):66-74. doi:10.1016/j.funeco.2008.10.008

71. Zucconi L, Cavallini G, Canini F. Trends in Antarctic soil fungal research in the context of environmental changes. *Braz J Microbiol*. 2024;55(2):1625-1634. doi:10.1007/s42770-024-01333-x

72. *Dry Valley Drilling Project*. 1st ed. American Geophysical Union (AGU); 1981. doi:10.1029/AR033

73. Fielding CR, Harwood DM, Winter DM, Francis JE. Neogene stratigraphy of Taylor Valley, Transantarctic Mountains, Antarctica: Evidence for climate dynamism and a vegetated Early Pliocene coastline of McMurdo Sound. *Glob Planet Change*. 2012;96-97:97-104. doi:10.1016/j.gloplacha.2010.09.003

74. Majewski W, Bart PJ, McGlannan AJ. Foraminiferal assemblages from ice-proximal paleo-settings in the Whales Deep Basin, eastern Ross Sea, Antarctica. *Palaeogeogr Palaeoclimatol Palaeoecol*. 2018;493:64-81. doi:10.1016/j.palaeo.2017.12.041

75. Ward BL, Barrett PJ, Vella P. Distribution and ecology of benthic foraminifera in McMurdo sound, antarctica. *Palaeogeogr Palaeoclimatol Palaeoecol*. 1987;58(3):139-153. doi:10.1016/0031-0182(87)90057-5

76. Habura A, Alexander SP, Hanes SD, Gooday AJ, Pawlowski J, Bowser SS. Distribution of two notodendrodid foraminiferal congeners in McMurdo Sound, Antarctica: an example of extreme regional endemism? *J Micropalaeontology*. 2024;43(2):337-347. doi:10.5194/jm-43-337-2024

77. Archer SDJ, Lee KC, Caruso T, et al. Airborne microbial transport limitation to isolated Antarctic soil habitats. *Nat Microbiol*. 2019;4(6):925-932. doi:10.1038/s41564-019-0370-4

78. Pearce DA, Bridge PD, Hughes KA, Sattler B, Psenner R, Russell NJ. Microorganisms in the atmosphere over Antarctica. *FEMS Microbiol Ecol*. 2009;69(2):143-157. doi:10.1111/j.1574-6941.2009.00706.x

79. Ríos-Castro R, Romero A, Aranguren R, et al. High-Throughput Sequencing of Environmental DNA as a Tool for Monitoring Eukaryotic Communities and Potential Pathogens in a Coastal Upwelling Ecosystem. *Front Vet Sci*. 2021;8. doi:10.3389/fvets.2021.765606

80. Berg G, Rybakova D, Fischer D, et al. Microbiome definition re-visited: old concepts and new challenges. *Microbiome*. 2020;8:103. doi:10.1186/s40168-020-00875-0

1399

1400

1401

Supplementary Files

This is a list of supplementary files associated with this preprint. Click to download.

- Additionalfile1OrthomosaicofDJPandchemicaldataofsampledpoints..docx
- Additionalfile2Fullaccountofmetadataandstatisticalanalysis.xlsx